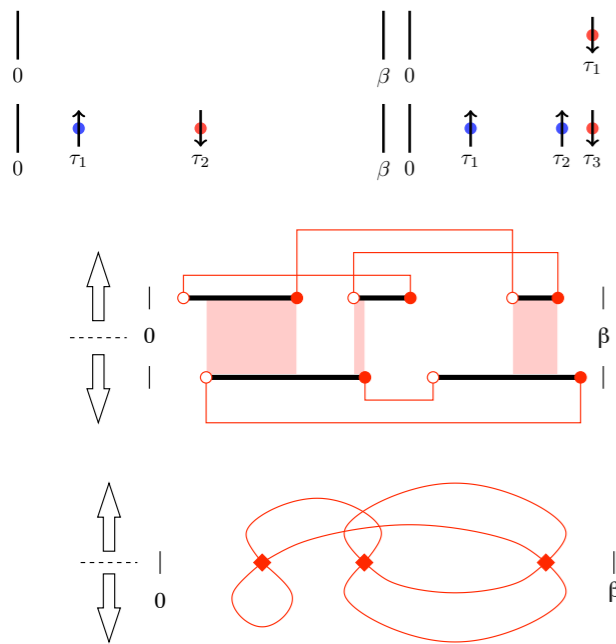


Continuous-Time Quantum Monte Carlo Algorithms

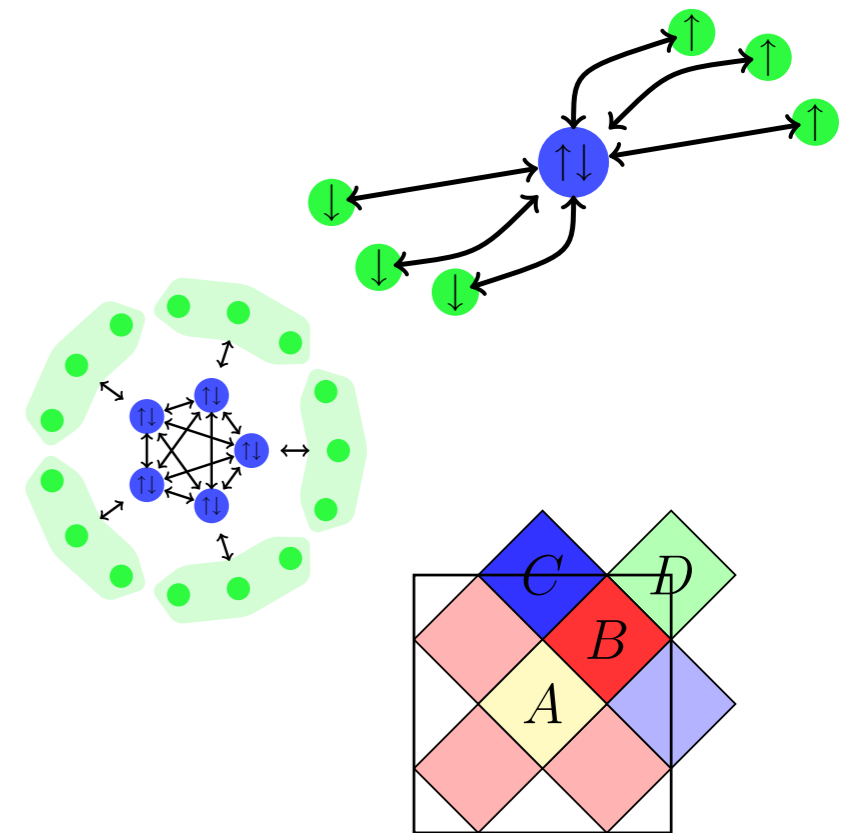


Emanuel Gull



January 7 2010

Funding: NSF-DMR-0705847



Overview

Quick introduction to the Dynamical Mean Field Theory (DMFT)

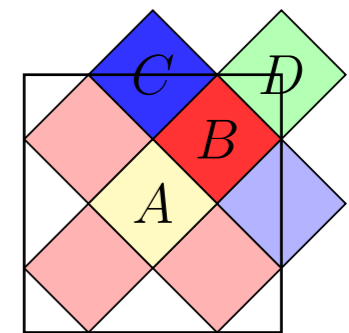
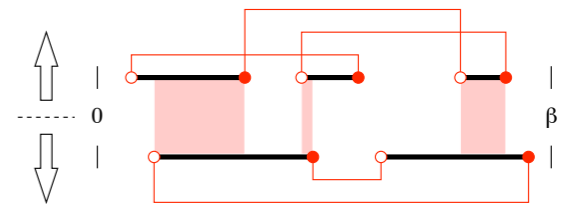
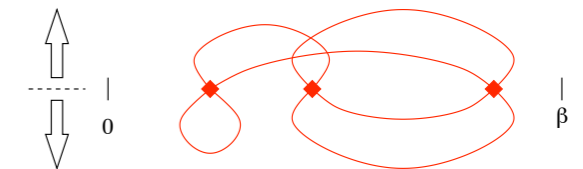
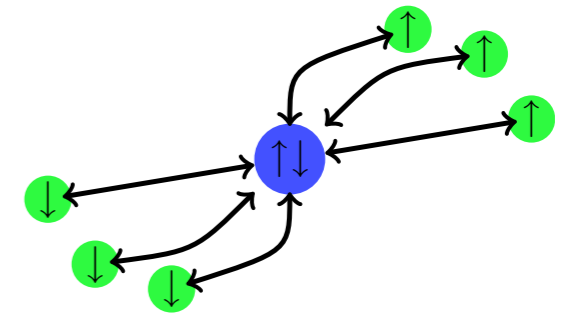
Continuous-Time Quantum Monte Carlo Methods and comparison to other methods

The Weak Coupling method

The Hybridization Expansion

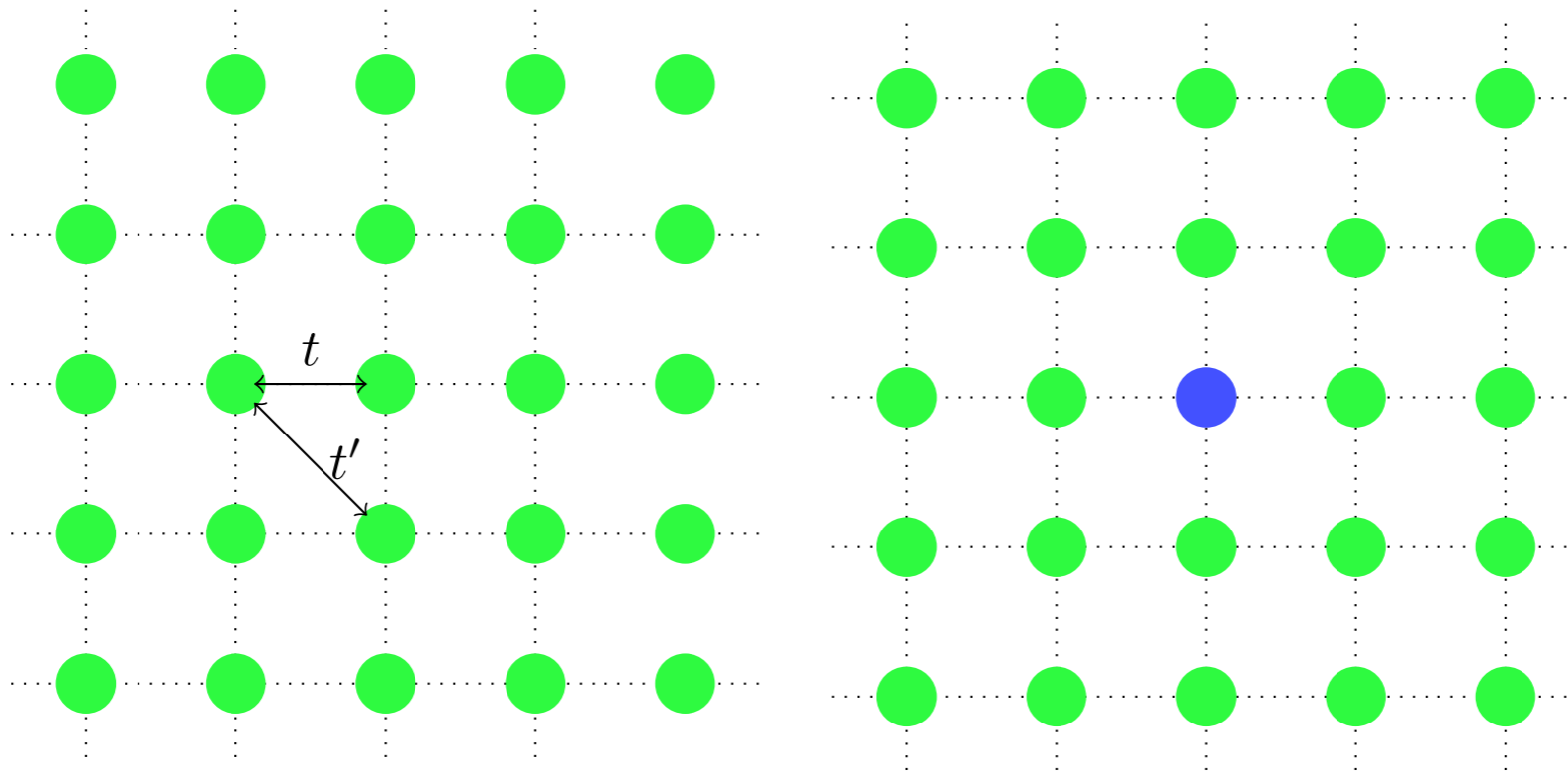
Continuous-Time Auxiliary Field impurity solver algorithm and large clusters

Some (very few) results (see P.Werner's talk for more applications)



DMFT and Impurity Problem

$$H = - \sum_{\langle ij \rangle, \sigma} t_{ij} (c_{i\sigma}^\dagger c_{j\sigma} + c_{j\sigma}^\dagger c_{i\sigma}) + U \sum_i n_{i\uparrow} n_{i\downarrow}.$$

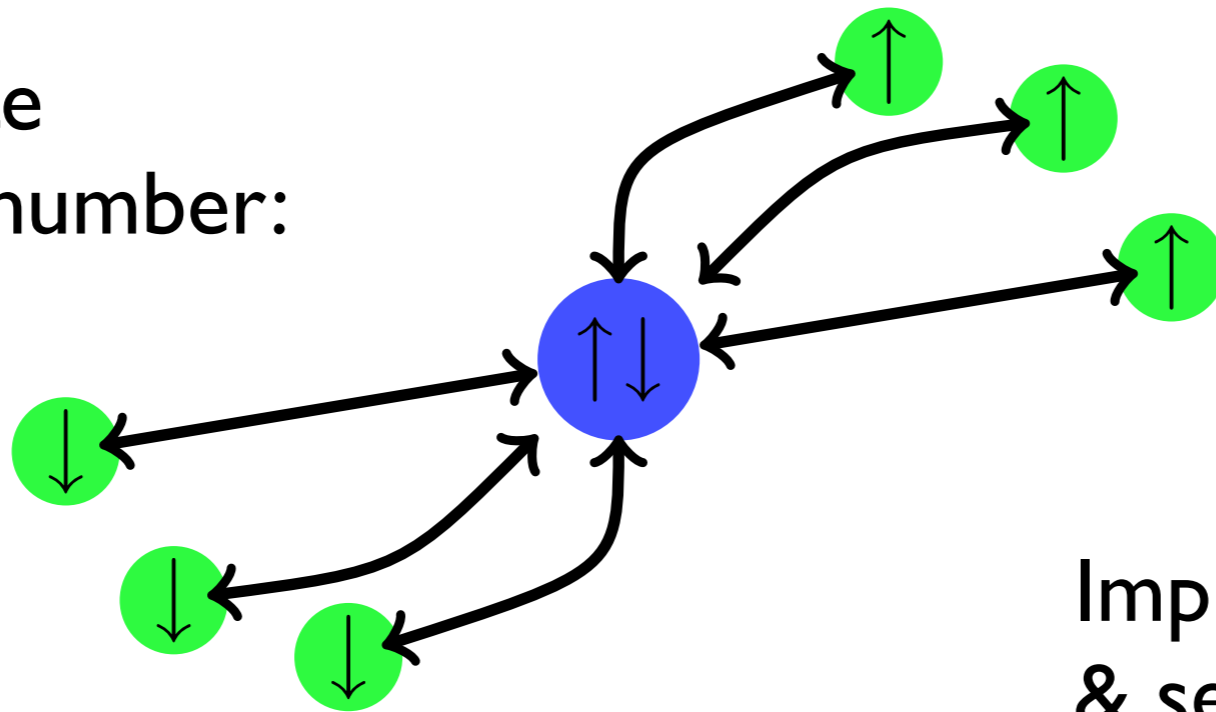


Impurity Problem: $S_{\text{eff}} = - \sum_{\sigma} \int \int_0^{\beta} d\tau d\tau' c_{\sigma}^{\dagger}(\tau) \mathcal{G}_{0\sigma}^{-1}(\tau - \tau') c_{\sigma}(\tau) + U \int_0^{\beta} d\tau n_{\uparrow}(\tau) n_{\downarrow}(\tau)$

Self Consistency: $G(i\omega_n) = \sum_{\vec{k} \in BZ} \frac{1}{i\omega_n + \mu - \epsilon(\vec{k}) - \Sigma(i\omega_n)}.$

DMFT and Impurity Problem

Limit of infinite
coordination number:

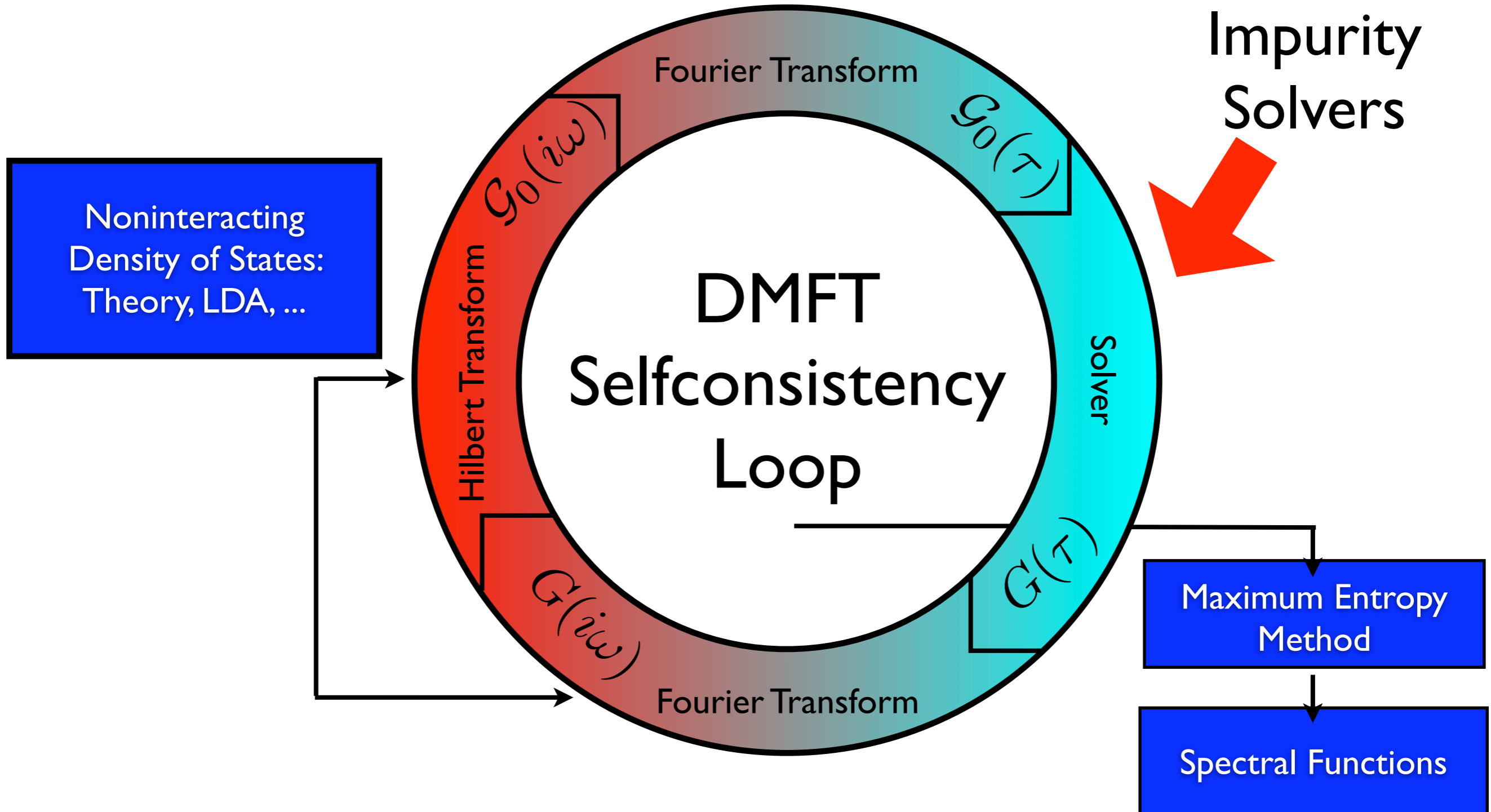


Impurity coupled to a bath
& self consistency
condition

Impurity Problem:
$$S_{\text{eff}} = - \sum_{\sigma} \int \int_0^{\beta} d\tau d\tau' c_{\sigma}^{\dagger}(\tau) \mathcal{G}_{0\sigma}^{-1}(\tau - \tau') c_{\sigma}(\tau) + U \int_0^{\beta} d\tau n_{\uparrow}(\tau) n_{\downarrow}(\tau)$$

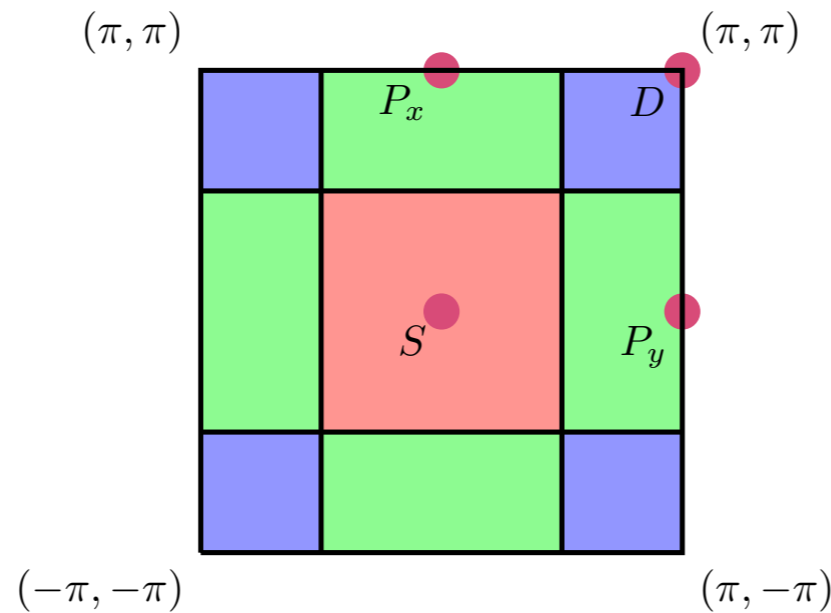
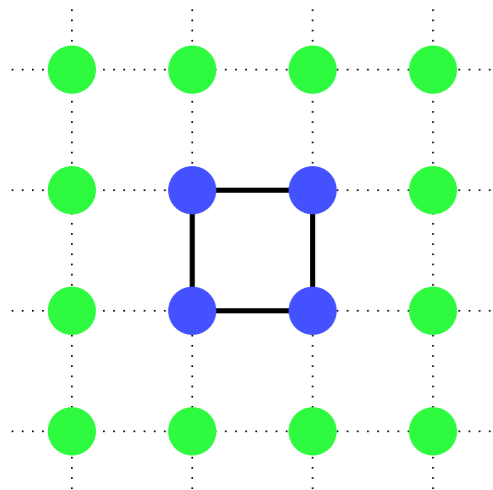
Self Consistency:
$$G(i\omega_n) = \sum_{\vec{k} \in BZ} \frac{1}{i\omega_n + \mu - \epsilon(\vec{k}) - \Sigma(i\omega_n)}.$$

DMFT Self Consistency



Cluster DMFT

Various variants developed by Lichtenstein *et al.*, Jarrell *et al.*, Kotliar *et al.*



Infinite coordination number:
momentum independent self
energy.

Dynamic Cluster Approximation
(DCA): reintroduce momentum
dependence to DMFT.

DCA self energy is chosen to be constant within patches of the Brillouin zone

Cluster impurity
problem

$$S_{\text{eff}} = - \int \int_0^\beta d\tau \sum_{ij\sigma} c_{i\sigma}^\dagger(\tau) \mathcal{G}_{ij,\sigma}^0(\tau - \tau')^{-1} c_{j\sigma}(\tau') + \int_0^\beta d\tau \sum_{j=1}^{N_c} U n_{j\uparrow}(\tau) n_{j\downarrow}(\tau)$$

Self consistency
condition

$$\Sigma_K = \mathcal{G}_K^0(i\omega_n)^{-1} - G_{\text{imp}}^{-1}$$

$$\bar{G}(K, i\omega_n) = \int_{\text{BZ patch}} \frac{dk}{i\omega_n + \mu - \epsilon(k) - \Sigma_K}$$

$$\mathcal{G}_K^0(i\omega_n)^{-1} = \Sigma_K + \bar{G}_K^{-1}(i\omega_n)$$

Hirsch Fye QMC Impurity Solver

$$H = - \sum_{\langle ij \rangle, \sigma} t_{ij} (c_{i\sigma}^\dagger c_{j\sigma} + c_{j\sigma}^\dagger c_{i\sigma}) + U \sum_i n_{i\uparrow} n_{i\downarrow}. \quad Z = \text{Tr} e^{-\beta H} = \text{Tr} \prod_{l=1}^L e^{-\Delta\tau (H_0 + V)}$$

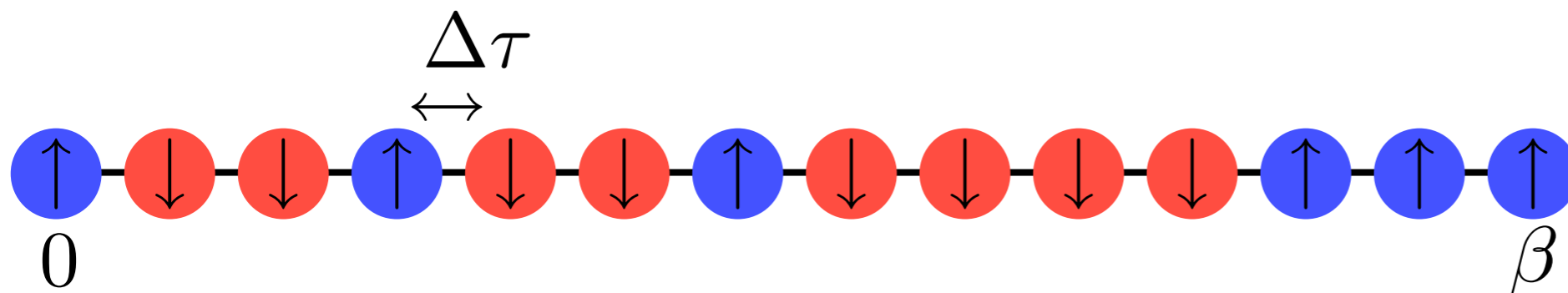
$$Z \simeq \prod_{l=1}^L e^{-\Delta\tau H_0} e^{-\Delta\tau V}$$

Trotter breakup: discretization of the integral, introduces Trotter errors

Auxiliary field decomposition

$$\exp \left[-\Delta\tau \left(U n_{\uparrow} n_{\downarrow} - \frac{1}{2} (n_{\uparrow} + n_{\downarrow}) \right) \right] = \frac{1}{2} \sum_{\sigma=\pm 1} \exp [\lambda \sigma (n_{\uparrow} - n_{\downarrow})]$$

$$\cosh(\lambda) = \exp(\Delta\tau U/2)$$



Sampling of partition function integral on discretized time slices

Continuous-Time Algorithms

Partition function in the interaction representation:

$$Z = \text{Tr} \left[e^{-\beta H_0} T_\tau e^{-\int_0^\beta d\tau V(\tau)} \right]$$

Expansion into perturbation series (powers of the interaction V):

$$Z = \sum_{k=0}^{\infty} \int d\tau_1 \cdots \int_{\tau_{k-1}}^{\beta} d\tau_k \text{Tr} \left[e^{-\beta H_0} e^{\tau_k H_0} (-V) \cdots e^{-(\tau_2 - \tau_1) H_0} (-V) e^{-\tau_1 H_0} \right].$$

Graphical representation of terms of the integral at different orders:

Continuous-Time Algorithms

Partition function in the interaction representation:

$$Z = \text{Tr} \left[e^{-\beta H_0} T_\tau e^{-\int_0^\beta d\tau V(\tau)} \right]$$

Expansion into perturbation series (powers of the interaction V):

$$Z = \sum_{k=0}^{\infty} \int d\tau_1 \cdots \int_{\tau_{k-1}}^{\beta} d\tau_k \text{Tr} \left[e^{-\beta H_0} e^{\tau_k H_0} (-V) \cdots e^{-(\tau_2 - \tau_1) H_0} (-V) e^{-\tau_1 H_0} \right].$$

Graphical representation of terms of the integral at different orders:

$$W_0 = \text{Tr} \left[e^{-\beta H_0} \right] \quad \text{a) } \left| \begin{array}{c} \text{---} \\ 0 \end{array} \right| \quad \left| \begin{array}{c} \text{---} \\ \beta \end{array} \right|$$

Continuous-Time Algorithms

Partition function in the interaction representation:

$$Z = \text{Tr} \left[e^{-\beta H_0} T_\tau e^{-\int_0^\beta d\tau V(\tau)} \right]$$

Expansion into perturbation series (powers of the interaction V):

$$Z = \sum_{k=0}^{\infty} \int d\tau_1 \cdots \int_{\tau_{k-1}}^{\beta} d\tau_k \text{Tr} \left[e^{-\beta H_0} e^{\tau_k H_0} (-V) \cdots e^{-(\tau_2 - \tau_1) H_0} (-V) e^{-\tau_1 H_0} \right].$$

Graphical representation of terms of the integral at different orders:

$$W_0 = \text{Tr} \left[e^{-\beta H_0} \right] \quad \text{a) } \left| \begin{array}{c} 0 \\ \beta \end{array} \right|$$

$$W_1(\tau_1) = \text{Tr} \left[e^{-(\beta - \tau_1) H_0} V e^{-\tau_1 H_0} \right] \quad \text{b) } \left| \begin{array}{c} 0 \\ \tau_1 \\ \beta \end{array} \right|$$



Continuous-Time Algorithms

Partition function in the interaction representation:

$$Z = \text{Tr} \left[e^{-\beta H_0} T_\tau e^{-\int_0^\beta d\tau V(\tau)} \right]$$

Expansion into perturbation series (powers of the interaction V):

$$Z = \sum_{k=0}^{\infty} \int d\tau_1 \cdots \int_{\tau_{k-1}}^{\beta} d\tau_k \text{Tr} \left[e^{-\beta H_0} e^{\tau_k H_0} (-V) \cdots e^{-(\tau_2 - \tau_1) H_0} (-V) e^{-\tau_1 H_0} \right].$$

Graphical representation of terms of the integral at different orders:

$$W_0 = \text{Tr} \left[e^{-\beta H_0} \right] \quad \text{a) } \begin{array}{|l} \beta \\ | \\ 0 \end{array}$$

$$W_1(\tau_1) = \text{Tr} \left[e^{-(\beta - \tau_1) H_0} V e^{-\tau_1 H_0} \right] \quad \text{b) } \begin{array}{|l} \beta \\ | \\ \tau_1 \\ | \\ 0 \end{array} \quad \bullet$$

$$W_2(\tau_1, \tau_2) = \text{Tr} \left[e^{-(\beta - \tau_1) H_0} V e^{-(\tau_1 - \tau_2) H_0} V e^{-\tau_2 H_0} \right] \quad \text{c) } \begin{array}{|l} \beta \\ | \\ \tau_2 \\ | \\ \tau_1 \\ | \\ 0 \end{array} \quad \bullet \quad \bullet$$

Continuous-Time Algorithms

Partition function in the interaction representation:

$$Z = \text{Tr} \left[e^{-\beta H_0} T_\tau e^{-\int_0^\beta d\tau V(\tau)} \right]$$

Expansion into perturbation series (powers of the interaction V):

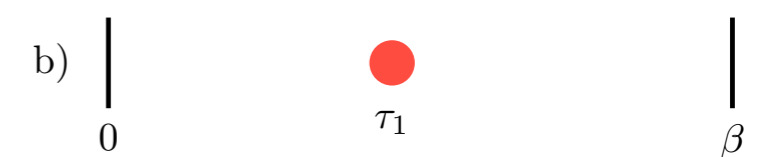
$$Z = \sum_{k=0}^{\infty} \int d\tau_1 \cdots \int_{\tau_{k-1}}^{\beta} d\tau_k \text{Tr} \left[e^{-\beta H_0} e^{\tau_k H_0} (-V) \cdots e^{-(\tau_2 - \tau_1) H_0} (-V) e^{-\tau_1 H_0} \right].$$

Graphical representation of terms of the integral at different orders:

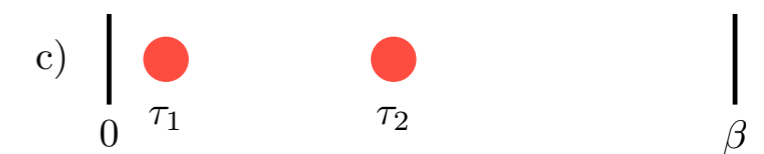
$$W_0 = \text{Tr} \left[e^{-\beta H_0} \right]$$



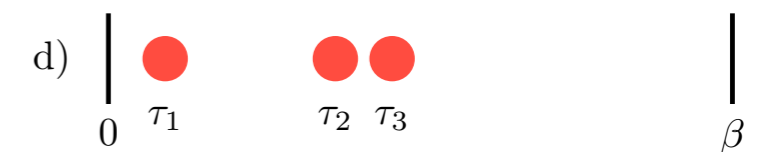
$$W_1(\tau_1) = \text{Tr} \left[e^{-(\beta - \tau_1) H_0} V e^{-\tau_1 H_0} \right]$$



$$W_2(\tau_1, \tau_2) = \text{Tr} \left[e^{-(\beta - \tau_1) H_0} V e^{-(\tau_1 - \tau_2) H_0} V e^{-\tau_2 H_0} \right]$$



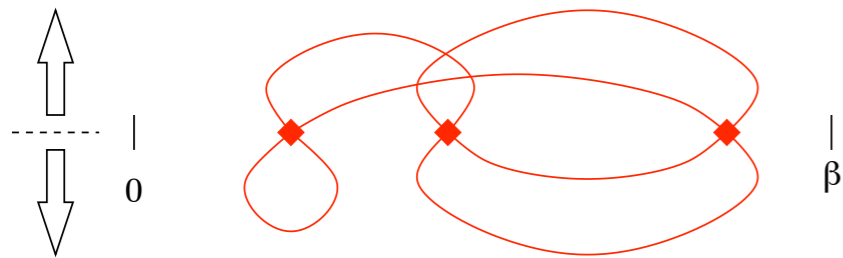
$$W_3(\tau_1, \tau_2, \tau_3) = \text{Tr} \left[e^{-(\beta - \tau_1) H_0} V e^{-(\tau_1 - \tau_2) H_0} V e^{-(\tau_2 - \tau_3) H_0} V e^{-\tau_3 H_0} \right]$$



Weak Coupling and Hybridization Expansion

$$Z = \sum_{k=0}^{\infty} \int d\tau_1 \cdots \int_{\tau_{k-1}}^{\beta} d\tau_k \text{Tr} \left[e^{-\beta H_0} e^{\tau_k H_0} (-V) \cdots e^{-(\tau_2 - \tau_1) H_0} (-V) e^{-\tau_1 H_0} \right].$$

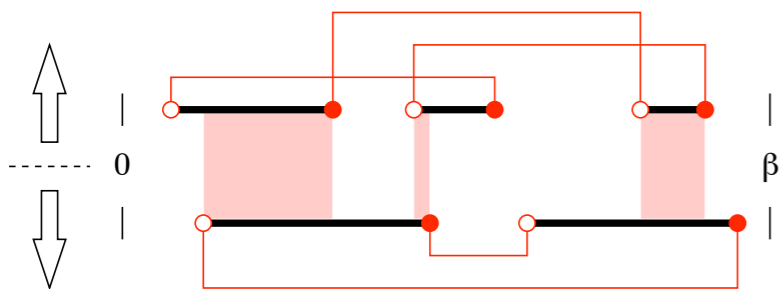
Two complementary approaches: Expansion in the interaction (e.g. the 'Hubbard U')



$$H = - \sum_{\langle ij \rangle, \sigma} t_{ij} (c_{i\sigma}^\dagger c_{j\sigma} + c_{j\sigma}^\dagger c_{i\sigma}) + U \sum_i n_{i\uparrow} n_{i\downarrow}.$$

Hopping exact

Expansion in the hybridization



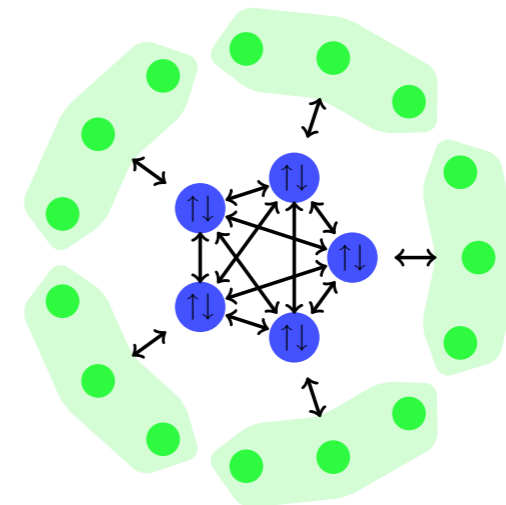
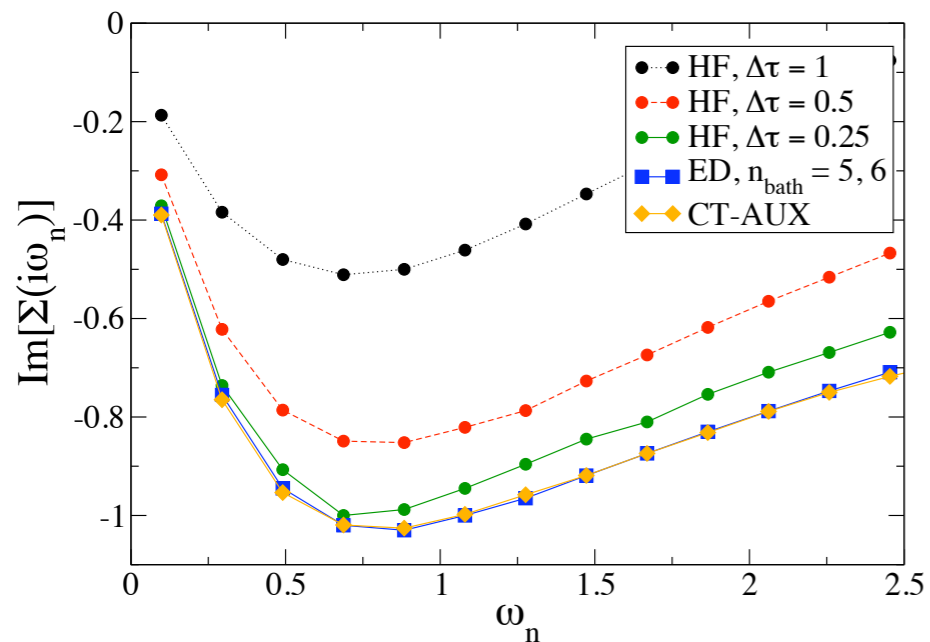
$$H = - \sum_{\langle ij \rangle, \sigma} t_{ij} (c_{i\sigma}^\dagger c_{j\sigma} + c_{j\sigma}^\dagger c_{i\sigma}) + U \sum_i n_{i\uparrow} n_{i\downarrow}.$$

Local Hamiltonian exact

Any analytical diagrammatic expansion can be converted into a QMC algorithm!

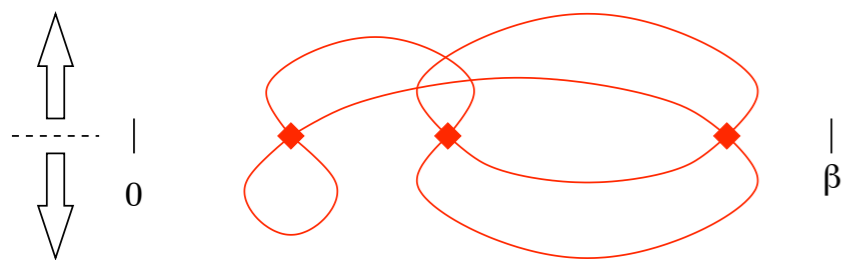
Advantages of Continuous Time QMC

No Approximations

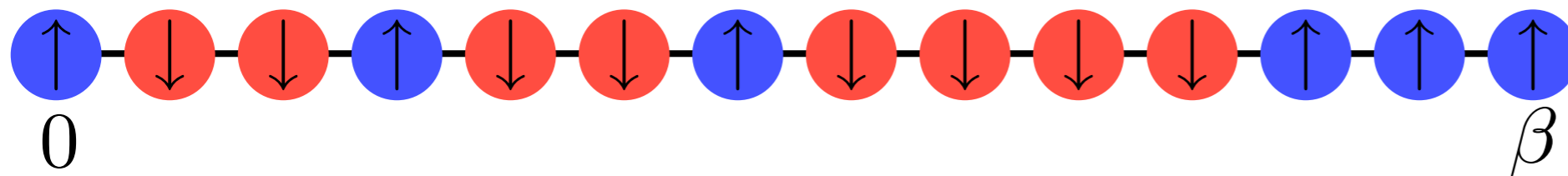


General interactions
(e.g. exchange & pair hopping), new physics

Speedup of about a factor of 10^3 :

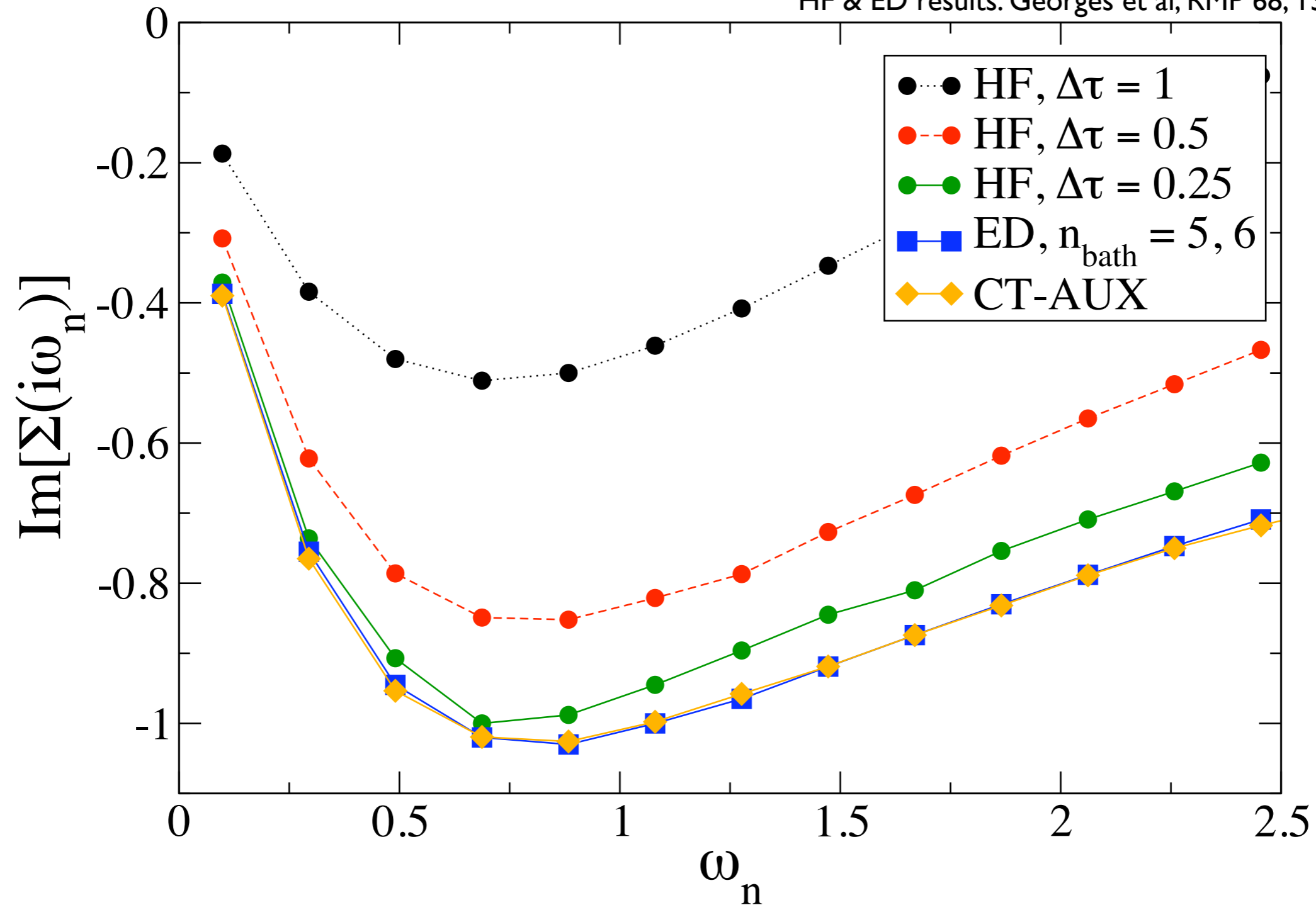


Intuitive picture: Smooth functions (diagrams) need to be approximated by a discretized version; resolution needs to be about 10 times larger than the features. Numerical effort is cubic ($O(N^3)$) for all algorithms



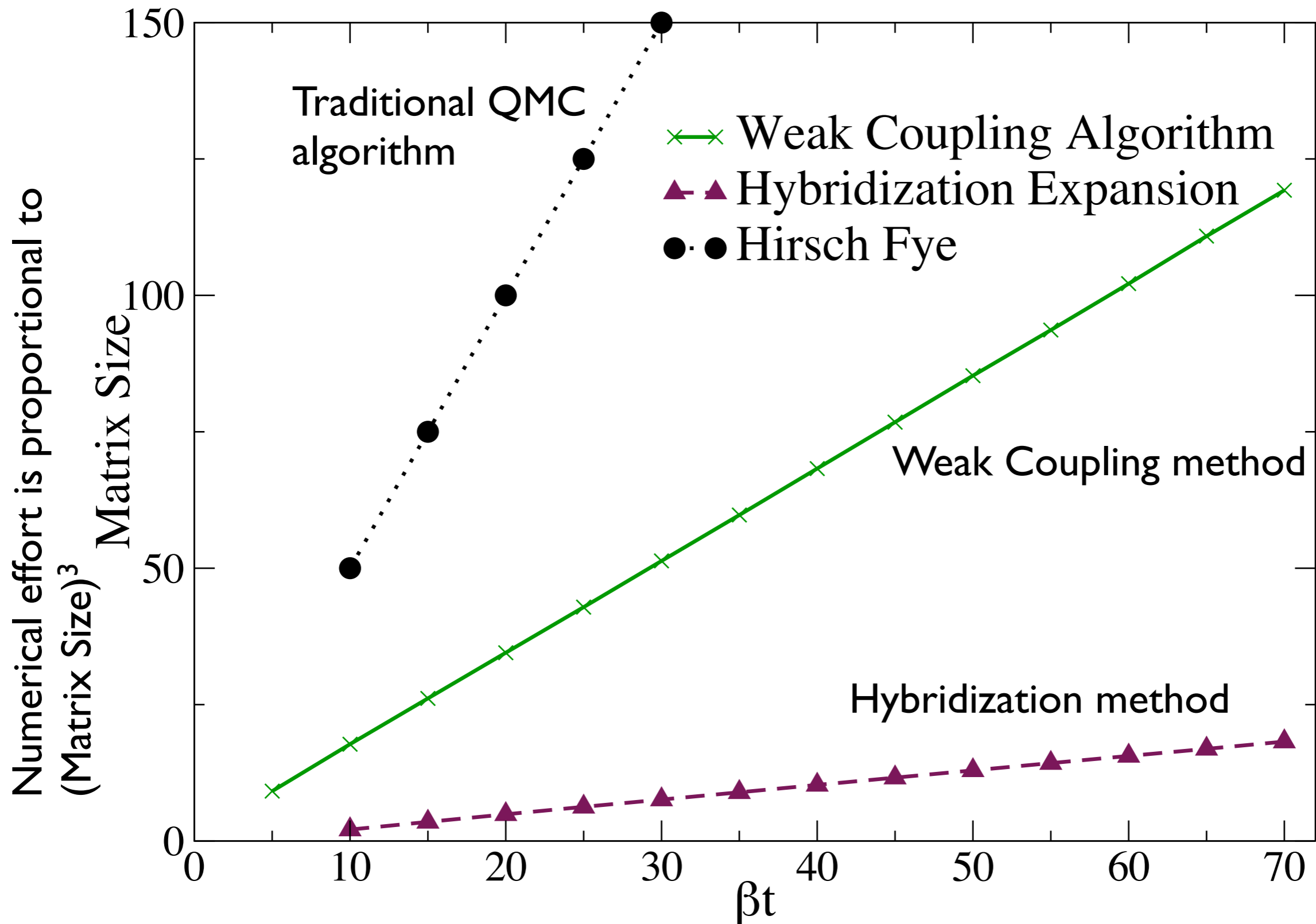
Discretization Errors

HF & ED results: Georges et al, RMP 68, 13 (1996)

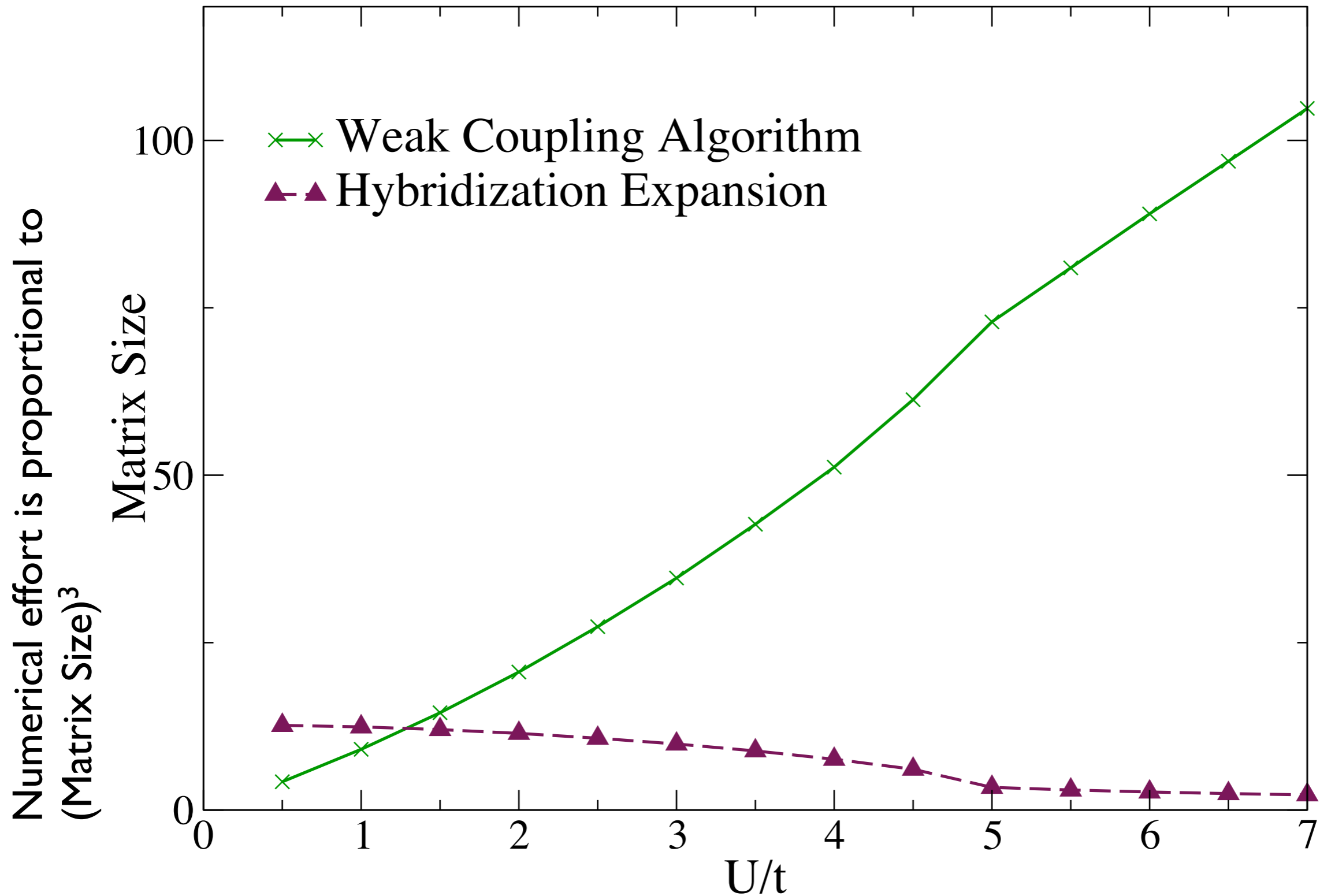


No discretization of the imaginary time interval as in Hirsch-Fye is necessary, extrapolation is avoided from the start.

Performance Comparison



Performance Comparison



Weak Coupling Algorithm

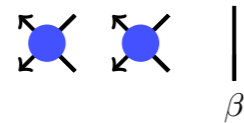
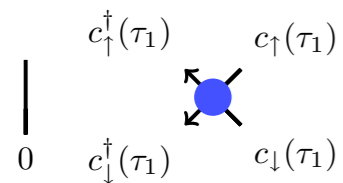
Weak coupling partition function expansion (SIAM):

$$\begin{aligned} \frac{Z}{Z_0} &= \sum_{k=0}^{\infty} \frac{(-U)^k}{k!} \iiint_0^{\beta} d\tau_1 \cdots d\tau_k \sum_{s_1 \cdots s_k} \prod_{\sigma} \langle T_{\tau} [n_{\sigma_1}(\tau_1) - \alpha_{s_1 \sigma_1}] \cdots [n_{\sigma_k}(\tau_k) - \alpha_{s_k \sigma_k}] \rangle \\ &= \sum_{k=0}^{\infty} \frac{(-U)^k}{k!} \iiint_0^{\beta} d\tau_1 \cdots d\tau_k \sum_{s_1 \cdots s_k} \prod_{\sigma} \det D_k^{\sigma} \end{aligned}$$

Weak Coupling Algorithm

Weak coupling partition function expansion (SIAM):

$$\begin{aligned} \frac{Z}{Z_0} &= \sum_{k=0}^{\infty} \frac{(-U)^k}{k!} \int \int \int_0^{\beta} d\tau_1 \cdots d\tau_k \sum_{s_1 \cdots s_k} \prod_{\sigma} \langle T_{\tau} [n_{\sigma_1}(\tau_1) - \alpha_{s_1 \sigma_1}] \cdots [n_{\sigma_k}(\tau_k) - \alpha_{s_k \sigma_k}] \rangle \\ &= \sum_{k=0}^{\infty} \frac{(-U)^k}{k!} \int \int \int_0^{\beta} d\tau_1 \cdots d\tau_k \sum_{s_1 \cdots s_k} \prod_{\sigma} \det D_k^{\sigma} \end{aligned}$$

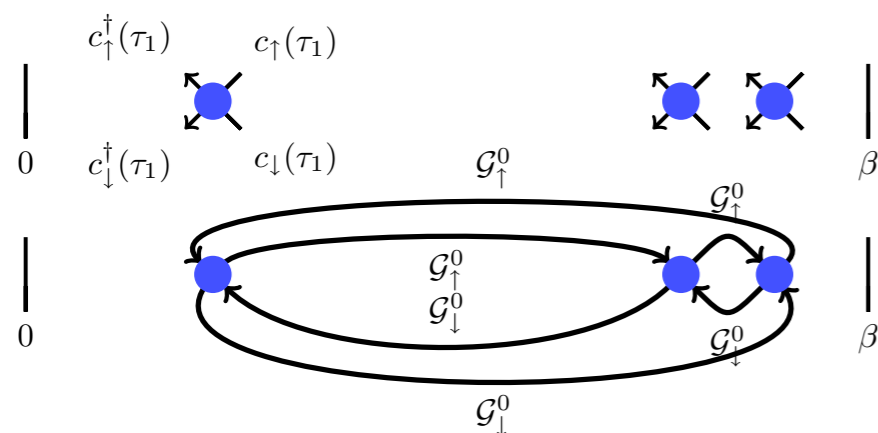


Location of interaction vertices

Weak Coupling Algorithm

Weak coupling partition function expansion (SIAM):

$$\begin{aligned} \frac{Z}{Z_0} &= \sum_{k=0}^{\infty} \frac{(-U)^k}{k!} \int \int \int_0^{\beta} d\tau_1 \cdots d\tau_k \sum_{s_1 \cdots s_k} \prod_{\sigma} \langle T_{\tau} [n_{\sigma_1}(\tau_1) - \alpha_{s_1 \sigma_1}] \cdots [n_{\sigma_k}(\tau_k) - \alpha_{s_k \sigma_k}] \rangle \\ &= \sum_{k=0}^{\infty} \frac{(-U)^k}{k!} \int \int \int_0^{\beta} d\tau_1 \cdots d\tau_k \sum_{s_1 \cdots s_k} \prod_{\sigma} \det D_k^{\sigma} \end{aligned}$$



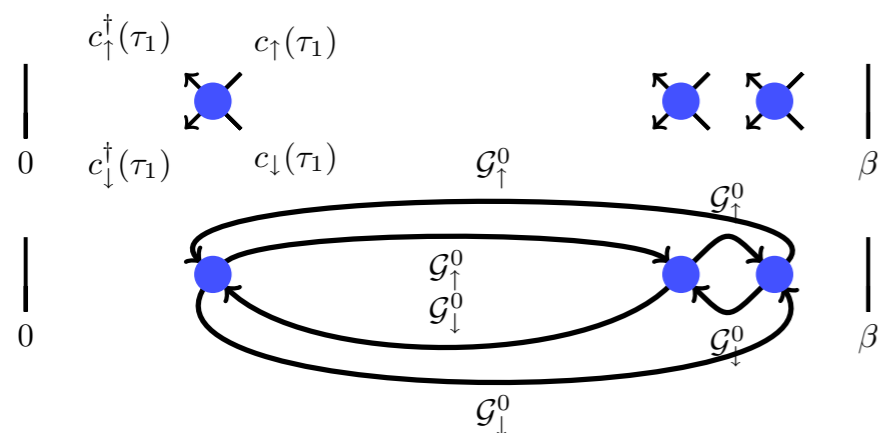
Location of interaction vertices

Green's function lines

Weak Coupling Algorithm

Weak coupling partition function expansion (SIAM):

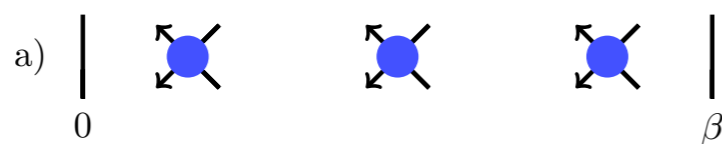
$$\begin{aligned} \frac{Z}{Z_0} &= \sum_{k=0}^{\infty} \frac{(-U)^k}{k!} \int \int \int_0^{\beta} d\tau_1 \cdots d\tau_k \sum_{s_1 \cdots s_k} \prod_{\sigma} \langle T_{\tau} [n_{\sigma_1}(\tau_1) - \alpha_{s_1 \sigma_1}] \cdots [n_{\sigma_k}(\tau_k) - \alpha_{s_k \sigma_k}] \rangle \\ &= \sum_{k=0}^{\infty} \frac{(-U)^k}{k!} \int \int \int_0^{\beta} d\tau_1 \cdots d\tau_k \sum_{s_1 \cdots s_k} \prod_{\sigma} \det D_k^{\sigma} \end{aligned}$$



Location of interaction vertices

Green's function lines

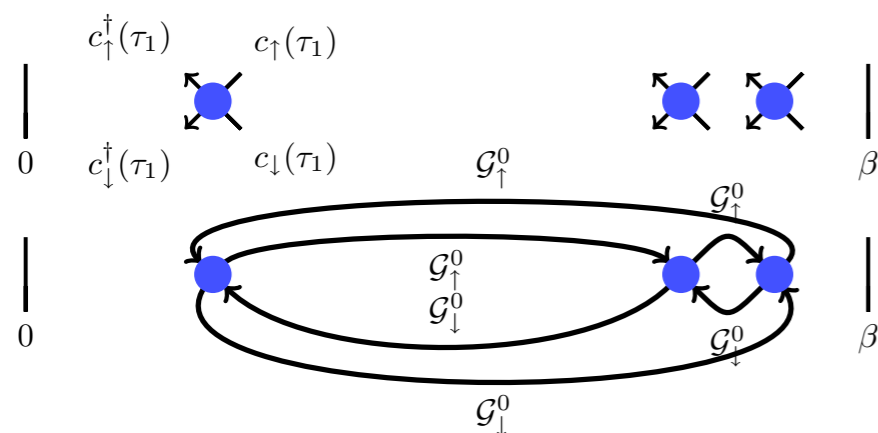
Monte Carlo
sampling
process:



Weak Coupling Algorithm

Weak coupling partition function expansion (SIAM):

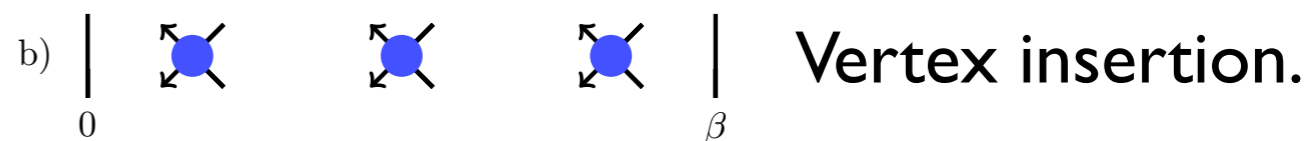
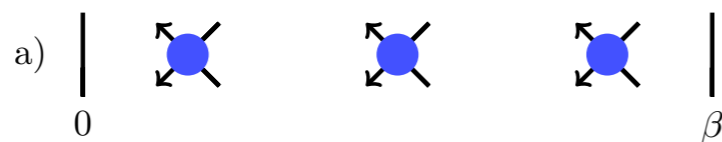
$$\begin{aligned} \frac{Z}{Z_0} &= \sum_{k=0}^{\infty} \frac{(-U)^k}{k!} \int \int \int_0^{\beta} d\tau_1 \cdots d\tau_k \sum_{s_1 \cdots s_k} \prod_{\sigma} \langle T_{\tau} [n_{\sigma_1}(\tau_1) - \alpha_{s_1 \sigma_1}] \cdots [n_{\sigma_k}(\tau_k) - \alpha_{s_k \sigma_k}] \rangle \\ &= \sum_{k=0}^{\infty} \frac{(-U)^k}{k!} \int \int \int_0^{\beta} d\tau_1 \cdots d\tau_k \sum_{s_1 \cdots s_k} \prod_{\sigma} \det D_k^{\sigma} \end{aligned}$$



Location of interaction vertices

Green's function lines

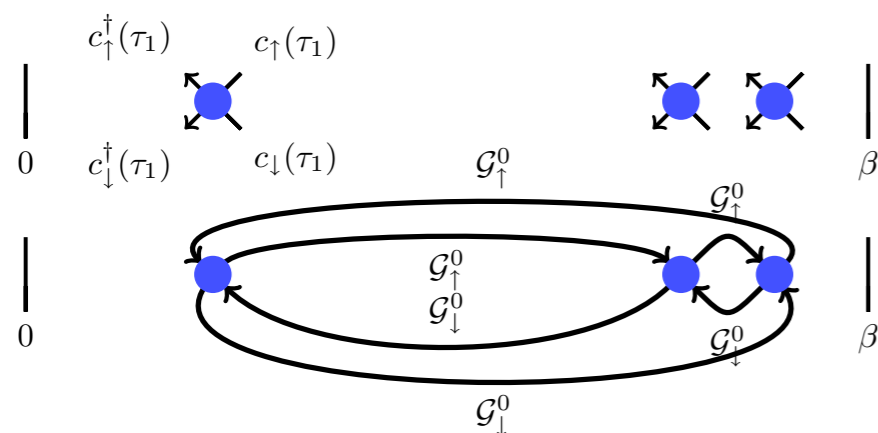
Monte Carlo sampling process:



Weak Coupling Algorithm

Weak coupling partition function expansion (SIAM):

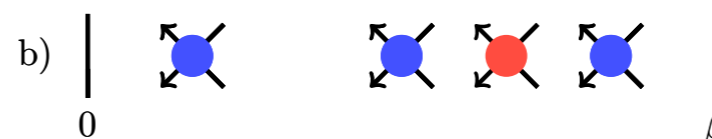
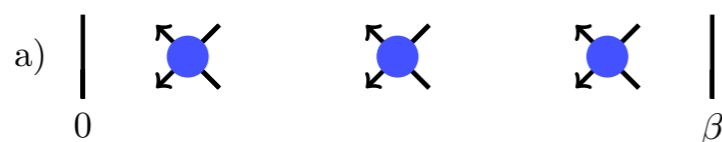
$$\begin{aligned} \frac{Z}{Z_0} &= \sum_{k=0}^{\infty} \frac{(-U)^k}{k!} \int \int \int_0^{\beta} d\tau_1 \cdots d\tau_k \sum_{s_1 \cdots s_k} \prod_{\sigma} \langle T_{\tau} [n_{\sigma_1}(\tau_1) - \alpha_{s_1 \sigma_1}] \cdots [n_{\sigma_k}(\tau_k) - \alpha_{s_k \sigma_k}] \rangle \\ &= \sum_{k=0}^{\infty} \frac{(-U)^k}{k!} \int \int \int_0^{\beta} d\tau_1 \cdots d\tau_k \sum_{s_1 \cdots s_k} \prod_{\sigma} \det D_k^{\sigma} \end{aligned}$$



Location of interaction vertices

Green's function lines

Monte Carlo sampling process:

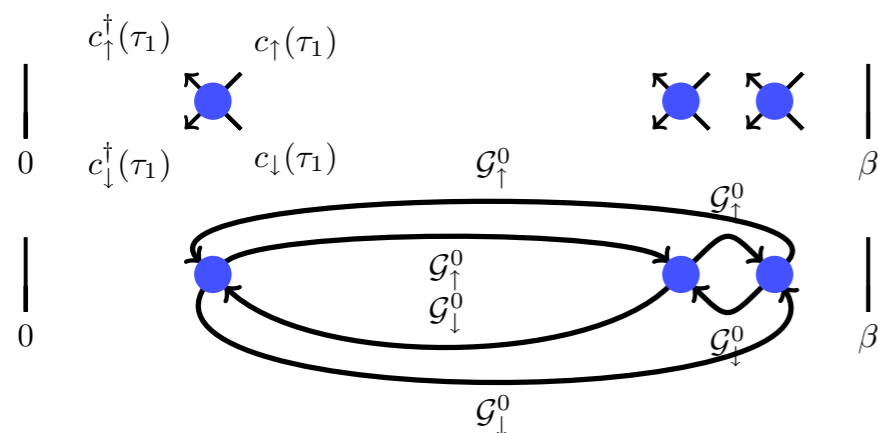


Vertex insertion.

Weak Coupling Algorithm

Weak coupling partition function expansion (SIAM):

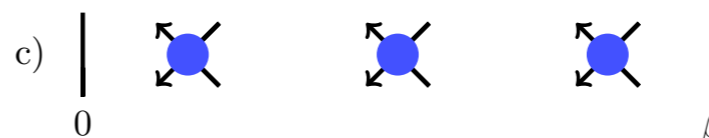
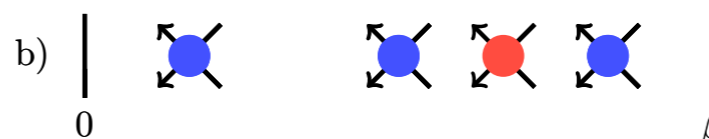
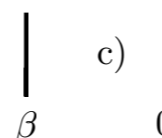
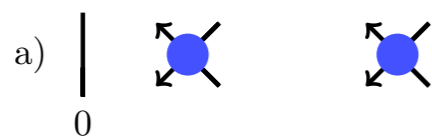
$$\begin{aligned} \frac{Z}{Z_0} &= \sum_{k=0}^{\infty} \frac{(-U)^k}{k!} \int \int \int_0^{\beta} d\tau_1 \cdots d\tau_k \sum_{s_1 \cdots s_k} \prod_{\sigma} \langle T_{\tau} [n_{\sigma_1}(\tau_1) - \alpha_{s_1 \sigma_1}] \cdots [n_{\sigma_k}(\tau_k) - \alpha_{s_k \sigma_k}] \rangle \\ &= \sum_{k=0}^{\infty} \frac{(-U)^k}{k!} \int \int \int_0^{\beta} d\tau_1 \cdots d\tau_k \sum_{s_1 \cdots s_k} \prod_{\sigma} \det D_k^{\sigma} \end{aligned}$$



Location of interaction vertices

Green's function lines

Monte Carlo sampling process:



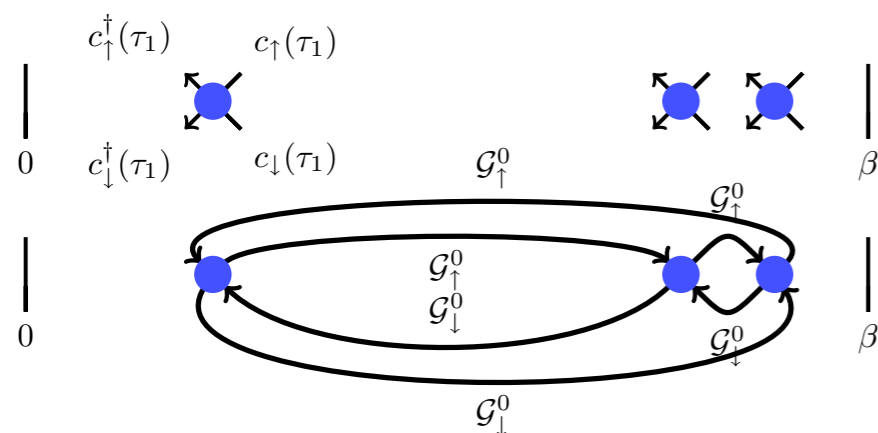
Vertex insertion.

Vertex removal.

Weak Coupling Algorithm

Weak coupling partition function expansion (SIAM):

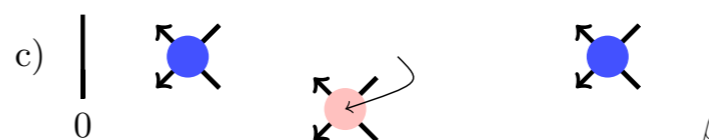
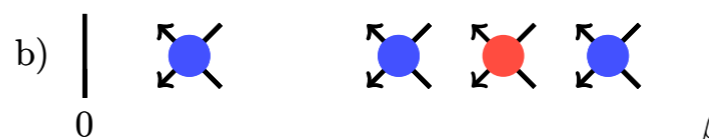
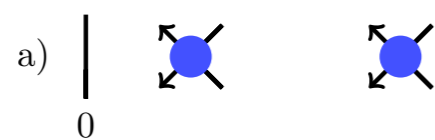
$$\begin{aligned} \frac{Z}{Z_0} &= \sum_{k=0}^{\infty} \frac{(-U)^k}{k!} \int \int \int_0^{\beta} d\tau_1 \cdots d\tau_k \sum_{s_1 \cdots s_k} \prod_{\sigma} \langle T_{\tau} [n_{\sigma_1}(\tau_1) - \alpha_{s_1 \sigma_1}] \cdots [n_{\sigma_k}(\tau_k) - \alpha_{s_k \sigma_k}] \rangle \\ &= \sum_{k=0}^{\infty} \frac{(-U)^k}{k!} \int \int \int_0^{\beta} d\tau_1 \cdots d\tau_k \sum_{s_1 \cdots s_k} \prod_{\sigma} \det D_k^{\sigma} \end{aligned}$$



Location of interaction vertices

Green's function lines

Monte Carlo sampling process:



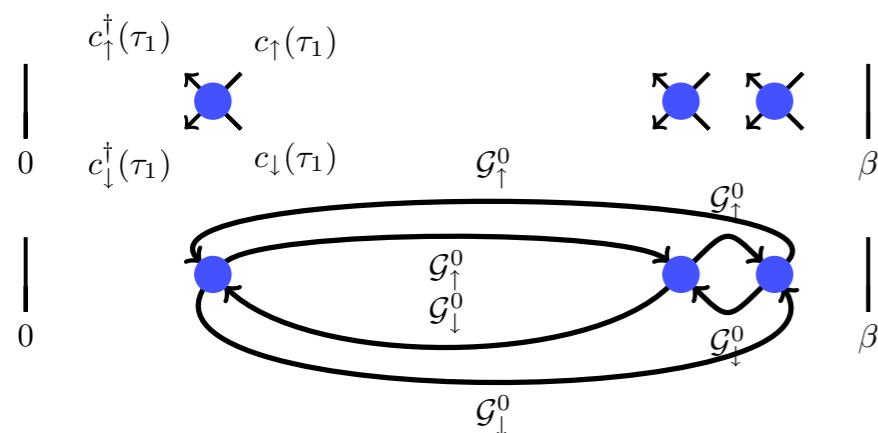
Vertex insertion.

Vertex removal.

Weak Coupling Algorithm

Weak coupling partition function expansion (SIAM):

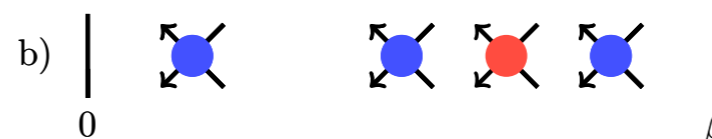
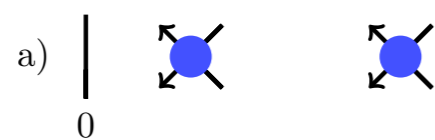
$$\begin{aligned} \frac{Z}{Z_0} &= \sum_{k=0}^{\infty} \frac{(-U)^k}{k!} \int \int \int_0^{\beta} d\tau_1 \cdots d\tau_k \sum_{s_1 \cdots s_k} \prod_{\sigma} \langle T_{\tau} [n_{\sigma_1}(\tau_1) - \alpha_{s_1 \sigma_1}] \cdots [n_{\sigma_k}(\tau_k) - \alpha_{s_k \sigma_k}] \rangle \\ &= \sum_{k=0}^{\infty} \frac{(-U)^k}{k!} \int \int \int_0^{\beta} d\tau_1 \cdots d\tau_k \sum_{s_1 \cdots s_k} \prod_{\sigma} \det D_k^{\sigma} \end{aligned}$$



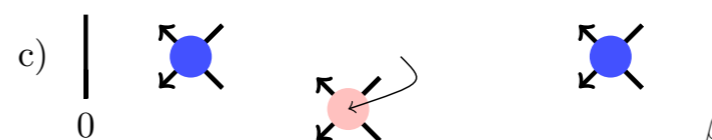
Location of interaction vertices

Green's function lines

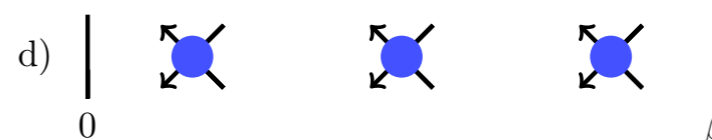
Monte Carlo sampling process:



Vertex insertion.



Vertex removal.

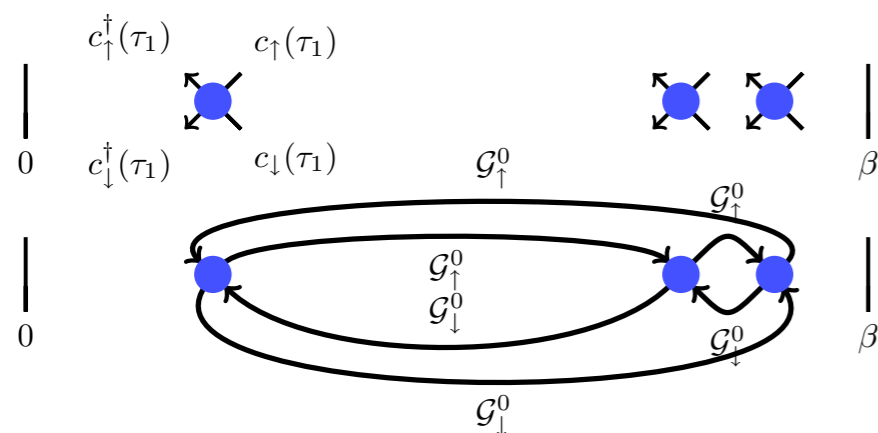


Vertex shift.

Weak Coupling Algorithm

Weak coupling partition function expansion (SIAM):

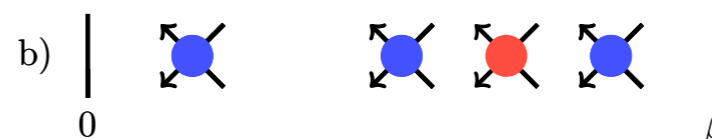
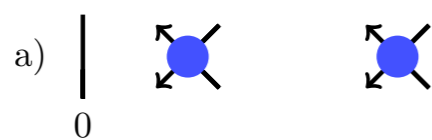
$$\begin{aligned} \frac{Z}{Z_0} &= \sum_{k=0}^{\infty} \frac{(-U)^k}{k!} \int \int \int_0^{\beta} d\tau_1 \cdots d\tau_k \sum_{s_1 \cdots s_k} \prod_{\sigma} \langle T_{\tau} [n_{\sigma_1}(\tau_1) - \alpha_{s_1 \sigma_1}] \cdots [n_{\sigma_k}(\tau_k) - \alpha_{s_k \sigma_k}] \rangle \\ &= \sum_{k=0}^{\infty} \frac{(-U)^k}{k!} \int \int \int_0^{\beta} d\tau_1 \cdots d\tau_k \sum_{s_1 \cdots s_k} \prod_{\sigma} \det D_k^{\sigma} \end{aligned}$$



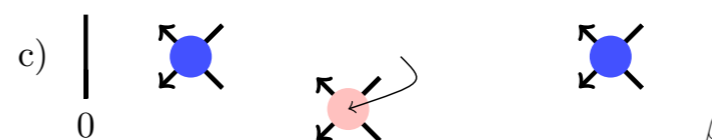
Location of interaction vertices

Green's function lines

Monte Carlo
sampling
process:



Vertex insertion.



Vertex removal.



Vertex shift.

Continuous-Time Auxiliary Field

Decoupling of the interaction with an auxiliary field:

$$1 - \frac{\beta U}{K} \left(n_{i\uparrow} n_{i\downarrow} - \frac{n_{i\uparrow} + n_{i\downarrow}}{2} \right) = \frac{1}{2} \sum_{s=\pm 1} \exp(\gamma s (n_{i\uparrow} - n_{i\downarrow})),$$

$$\cosh(\gamma) = 1 + \frac{U\beta}{2K}.$$

Partition function expansion in the interaction representation:

$$Z = \sum_{k=0}^{\infty} \sum_{s_1, \dots, s_k = \pm 1} \int_0^{\beta} d\tau_1 \cdots \int_{\tau_{k-1}}^{\beta} d\tau_k \left(\frac{K}{2\beta} \right)^k Z_k(\{s_k, \tau_k\}),$$

$$Z_k(\{s_i, \tau_i\}) \equiv \text{Tr} \prod_{i=k}^1 \exp(-\Delta\tau_i H_0) \exp(s_i \gamma (n_{\uparrow} - n_{\downarrow})).$$

Continuous-Time Auxiliary Field

Decoupling of the interaction with an auxiliary field:

$$1 - \frac{\beta U}{K} \left(n_{i\uparrow} n_{i\downarrow} - \frac{n_{i\uparrow} + n_{i\downarrow}}{2} \right) = \frac{1}{2} \sum_{s=\pm 1} \exp(\gamma s (n_{i\uparrow} - n_{i\downarrow})),$$

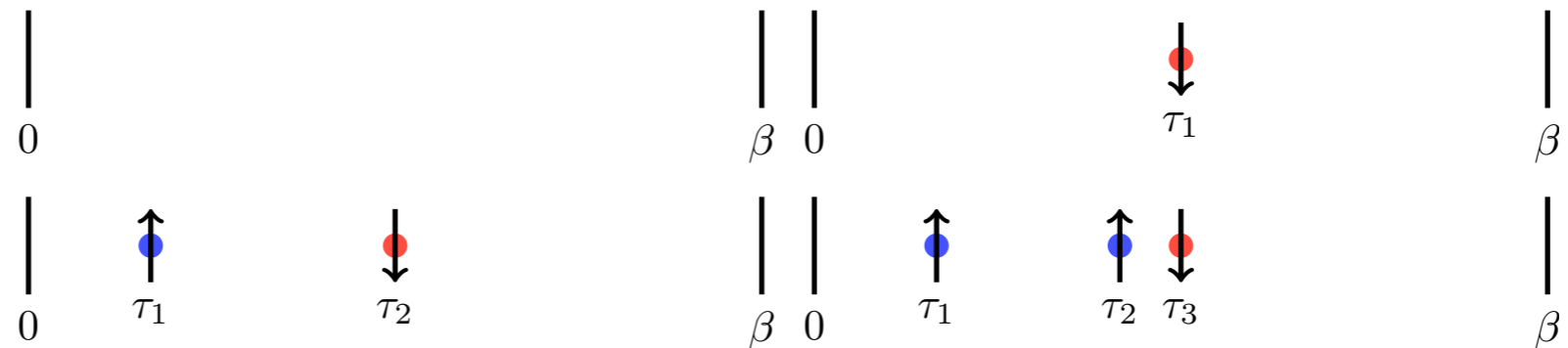
$$\cosh(\gamma) = 1 + \frac{U\beta}{2K}.$$

Partition function expansion in the interaction representation:

$$Z = \sum_{k=0}^{\infty} \sum_{s_1, \dots, s_k = \pm 1} \int_0^{\beta} d\tau_1 \cdots \int_{\tau_{k-1}}^{\beta} d\tau_k \left(\frac{K}{2\beta} \right)^k Z_k(\{s_k, \tau_k\}),$$

$$Z_k(\{s_i, \tau_i\}) \equiv \text{Tr} \prod_{i=k}^1 \exp(-\Delta\tau_i H_0) \exp(s_i \gamma (n_{\uparrow} - n_{\downarrow})).$$

Diagrams of the partition function:



Continuous-Time Auxiliary Field

Decoupling of the interaction with an auxiliary field:

$$1 - \frac{\beta U}{K} \left(n_{i\uparrow} n_{i\downarrow} - \frac{n_{i\uparrow} + n_{i\downarrow}}{2} \right) = \frac{1}{2} \sum_{s=\pm 1} \exp(\gamma s (n_{i\uparrow} - n_{i\downarrow})),$$

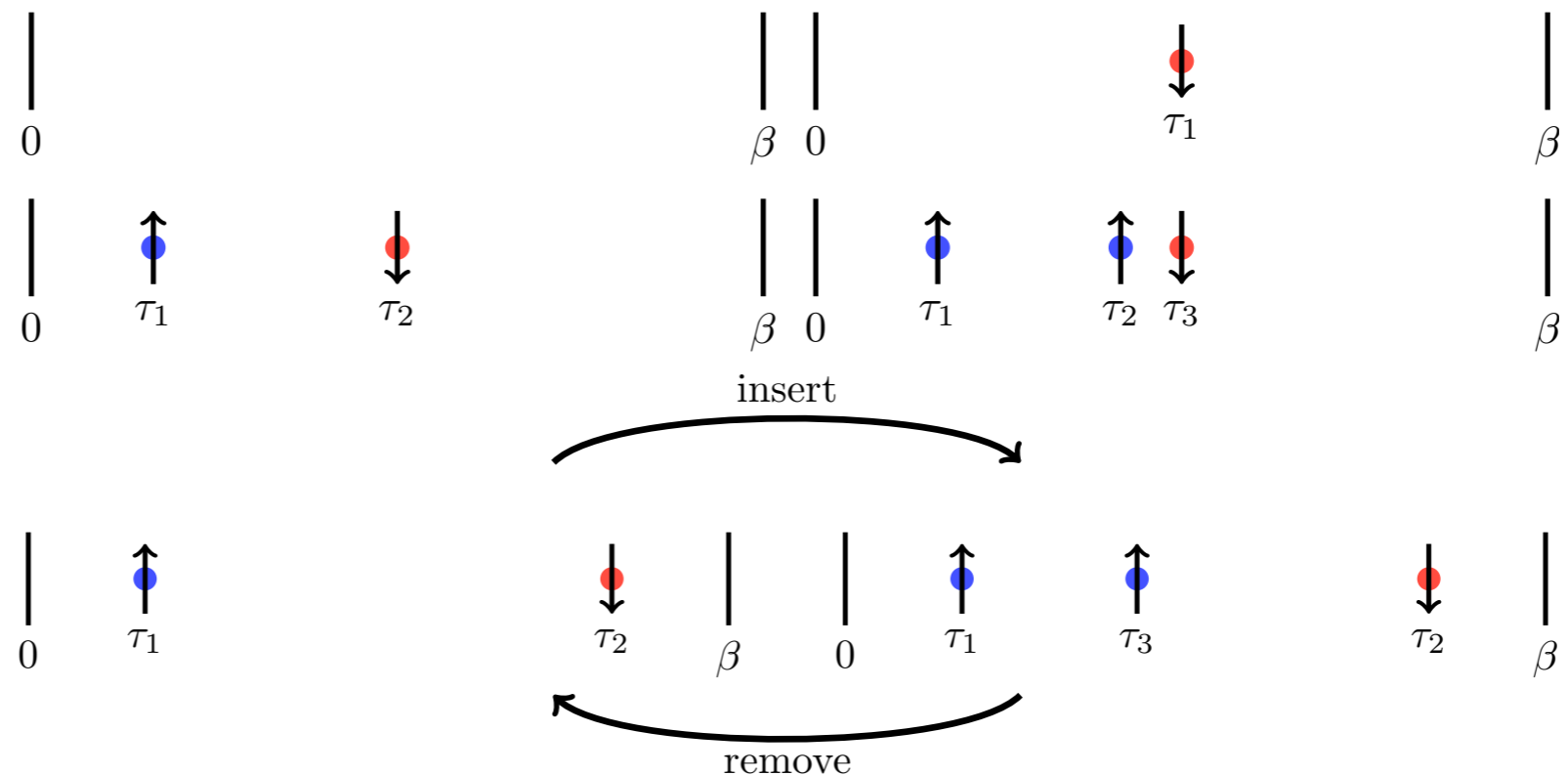
$$\cosh(\gamma) = 1 + \frac{U\beta}{2K}.$$

Partition function expansion in the interaction representation:

$$Z = \sum_{k=0}^{\infty} \sum_{s_1, \dots, s_k = \pm 1} \int_0^{\beta} d\tau_1 \cdots \int_{\tau_{k-1}}^{\beta} d\tau_k \left(\frac{K}{2\beta} \right)^k Z_k(\{s_k, \tau_k\}),$$

$$Z_k(\{s_i, \tau_i\}) \equiv \text{Tr} \prod_{i=k}^1 \exp(-\Delta\tau_i H_0) \exp(s_i \gamma (n_{\uparrow} - n_{\downarrow})).$$

Diagrams of the partition function:



Monte Carlo Sampling:

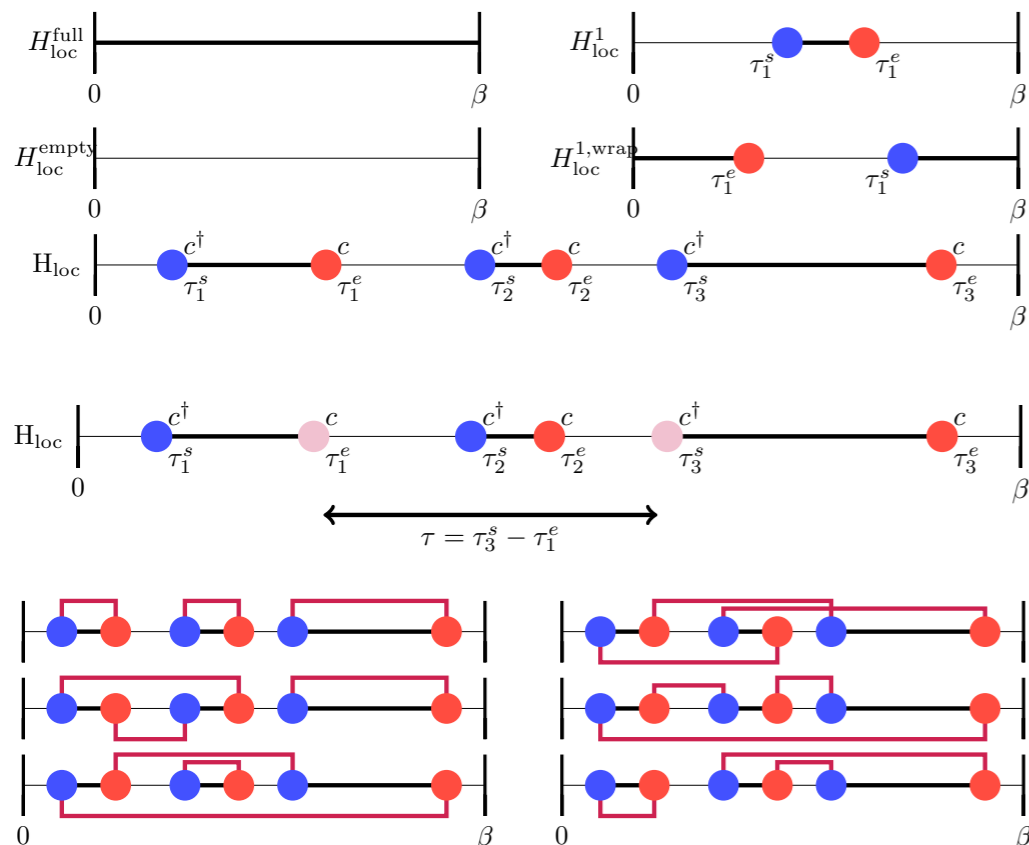
Hybridization Expansion

Expansion in the interaction representation, where $V = H_{mix}$, $H_0 = H_{loc}$. Density - density interactions.

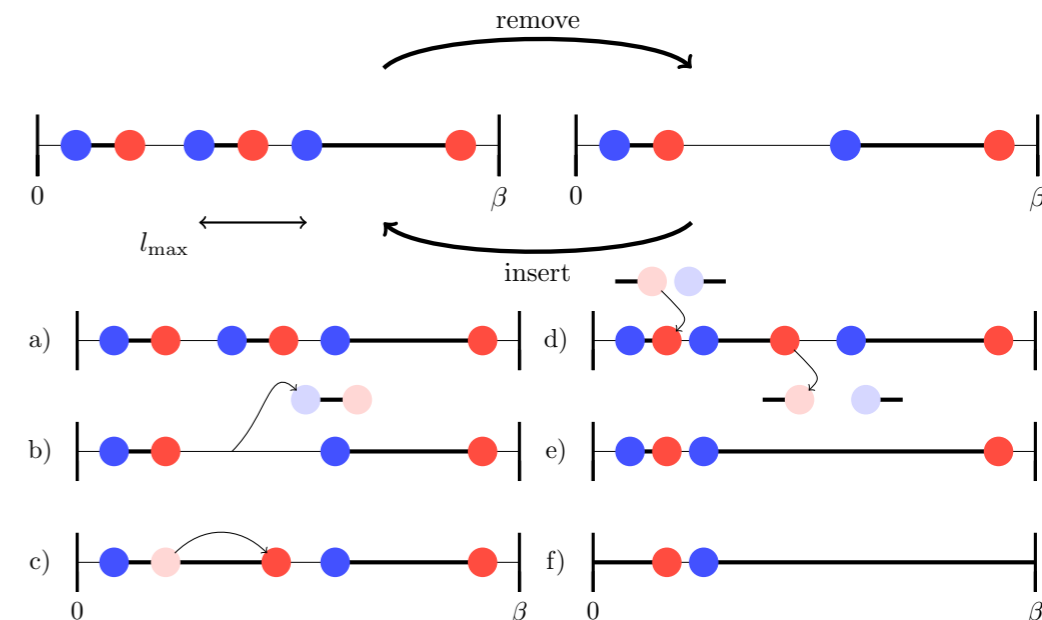
$$Z = \text{Tr} e^{-\beta H} = \text{Tr} \left[e^{-\beta H_0} T_\tau e^{-\int_0^\beta d\tau H_{mix}(\tau)} \right]$$

$$= \sum_{k=0}^{\infty} \int d\tau_1 \cdots \int_{\tau_{k-1}}^{\beta} d\tau_k \text{Tr} \left[e^{-\beta H_0} e^{\tau_k H_0} (-H_{mix}) \cdots e^{-(\tau_2 - \tau_1) H_0} (-H_{mix}) e^{-\tau_1 H_0} \right]$$

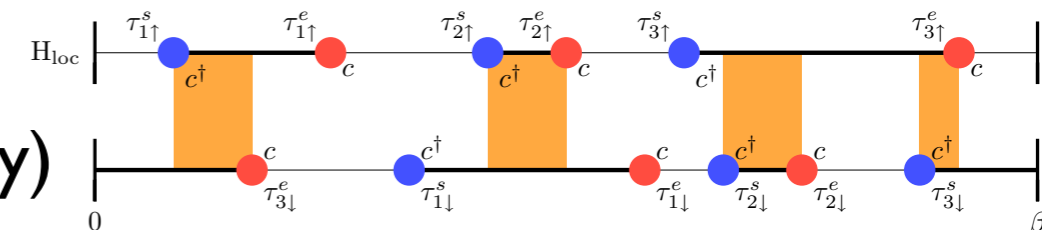
Configurations



Sampling Process



Interactions (density density)

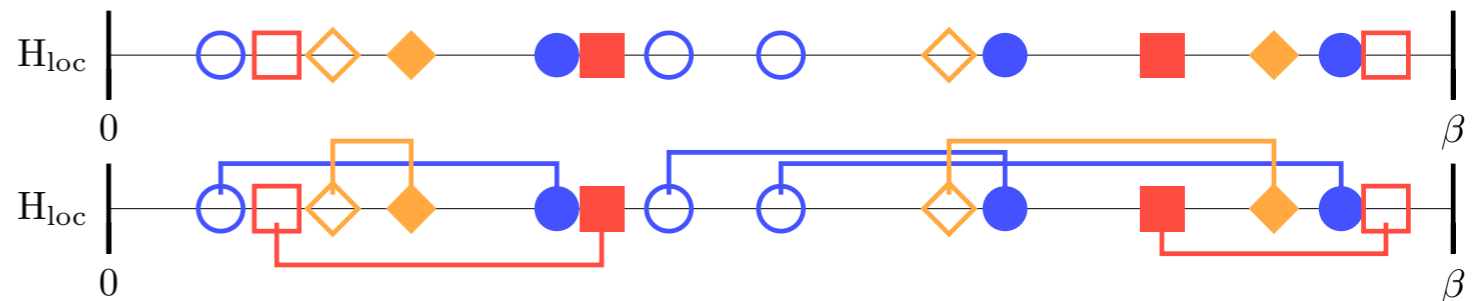


Hybridization - General Interactions

More complicated interactions (clusters, multiorbital, phonons, ...)?

Configuration of H_{loc}

Configuration of V

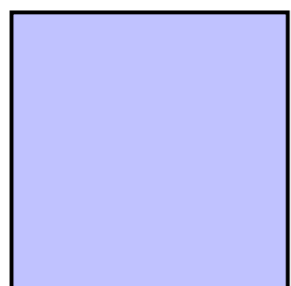


$$Z = \text{Tr} e^{-\beta H} = \text{Tr} \left[e^{-\beta H_0} T_\tau e^{-\int_0^\beta d\tau H_{\text{mix}}(\tau)} \right]$$

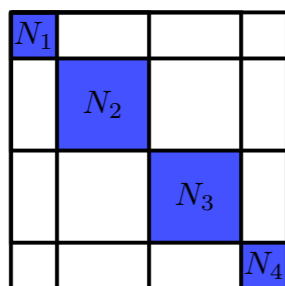
$$= \sum_{k=0}^{\infty} \int d\tau_1 \cdots \int_{\tau_{k-1}}^{\beta} d\tau_k \text{Tr} \left[e^{-\beta H_0} e^{\tau_k H_0} (-H_{\text{mix}}) \cdots e^{-(\tau_2 - \tau_1) H_0} (-H_{\text{mix}}) e^{-\tau_1 H_0} \right]$$

Matrix exponentials

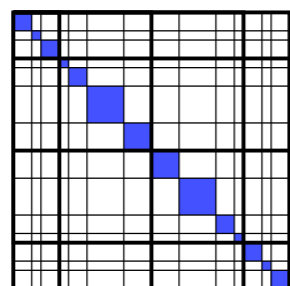
occupation number basis $[H_{loc}, S_z] = 0 = [H_{loc}, N]$ further symmetries



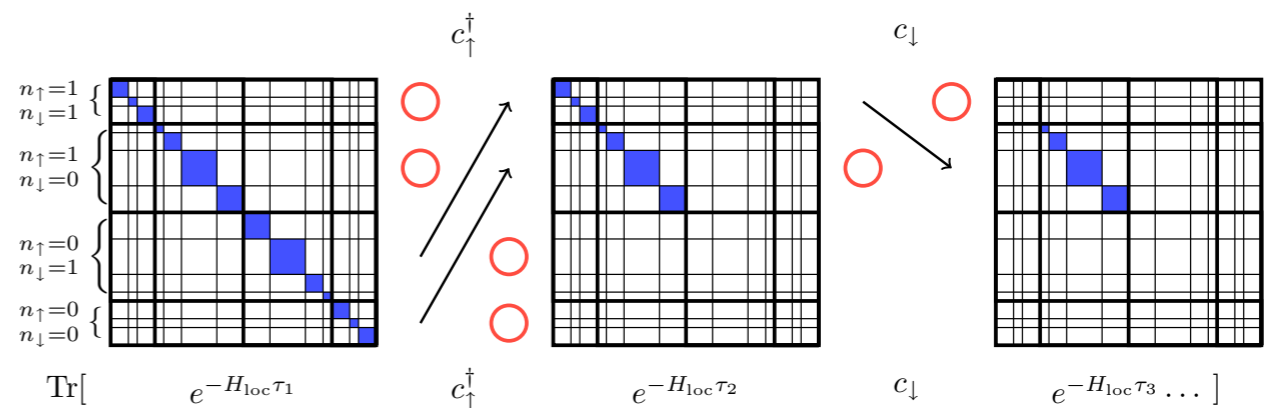
H_{loc}



H_{loc}

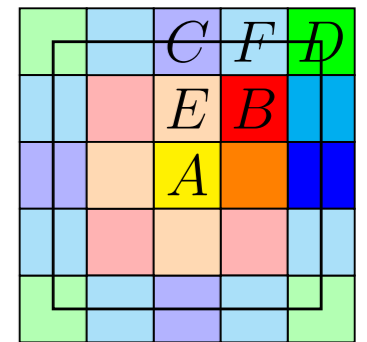
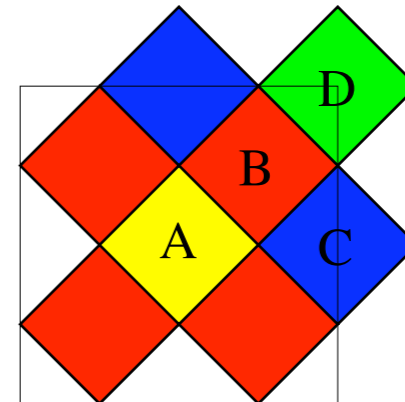
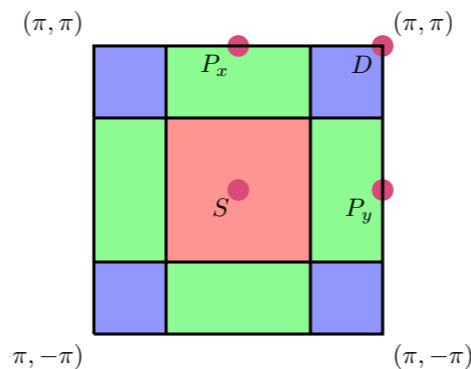


H_{loc}

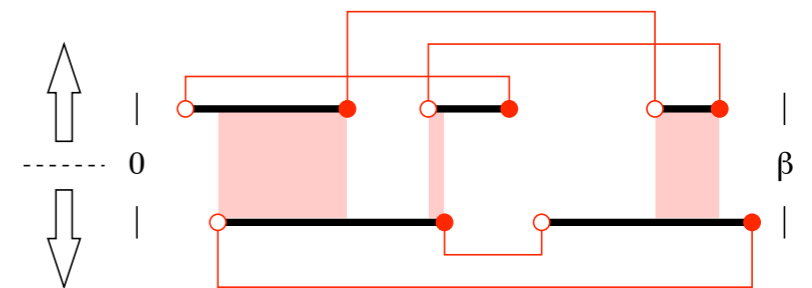


Choosing the appropriate Algorithm

Large cluster calculations:
Continuous-time auxiliary field method (up to 10x10 clusters)

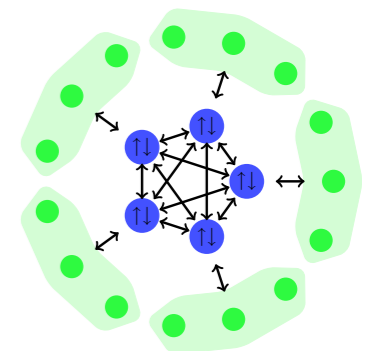


Problems with density density interactions, many orbitals: **Hybridization expansion** (linear in the number of orbitals)



Problems with general but weak interactions: **Weak Coupling expansion**

Problems with general interactions but few orbitals: **Hybridization expansion.**

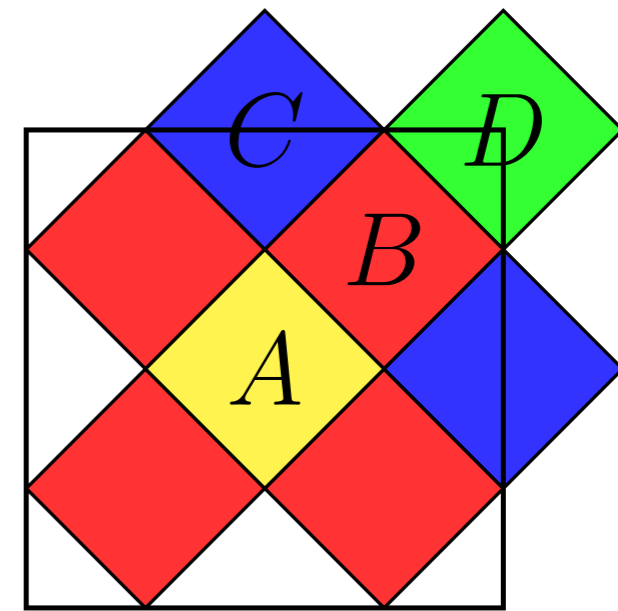
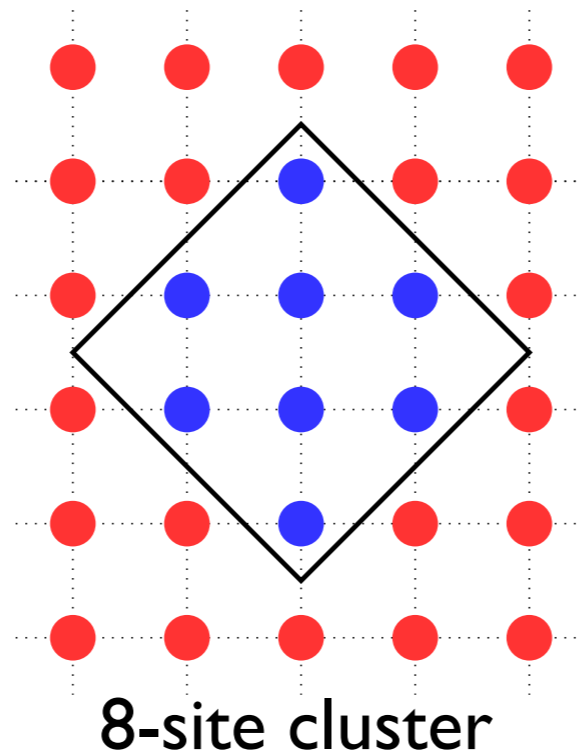
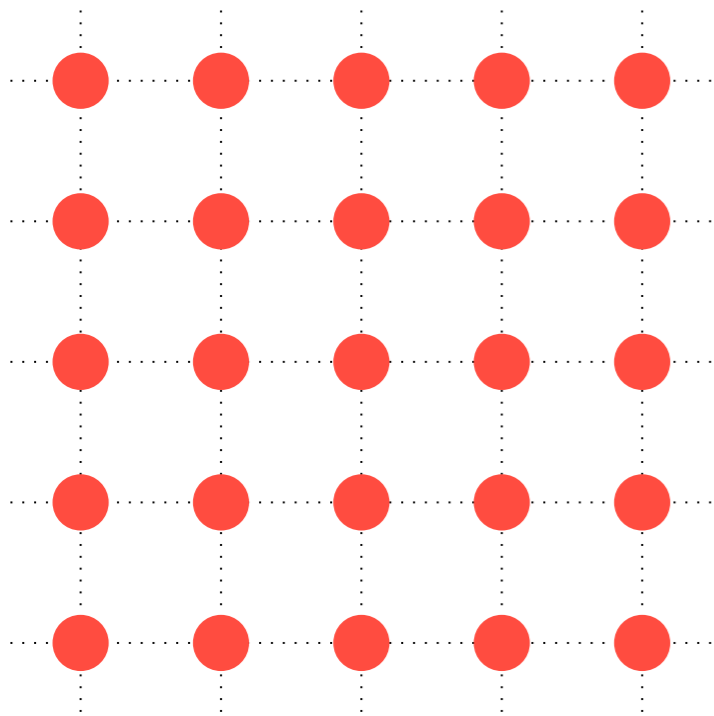


Cluster Dynamical Mean Field Theory

Maier et al., Rev. Mod. Phys. 77, 1027 (2005)

Hubbard model on
2d square lattice:

$$H = - \sum_{\langle ij \rangle, \sigma} t_{ij} (c_{i\sigma}^\dagger c_{j\sigma} + c_{j\sigma}^\dagger c_{i\sigma}) + U \sum_i n_{i\uparrow} n_{i\downarrow}.$$



Tiling of the BZ

DCA: Hettler et al.,
Phys. Rev. B 58, R 7475 (1998)

Restriction to paramagnetic bath

$$\epsilon_p = -2t(\cos(p_x) + \cos(p_y)) - 4t' \cos(p_x) \cos(p_y)$$

DCA self energy is chosen to be constant within patches of the Brillouin zone.

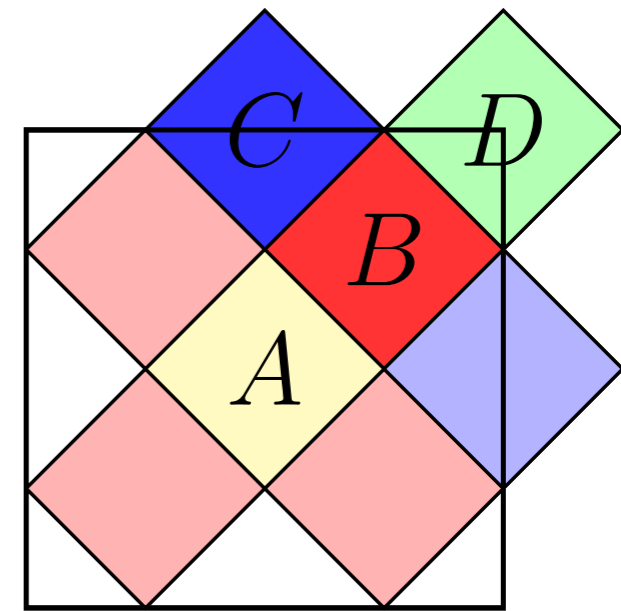
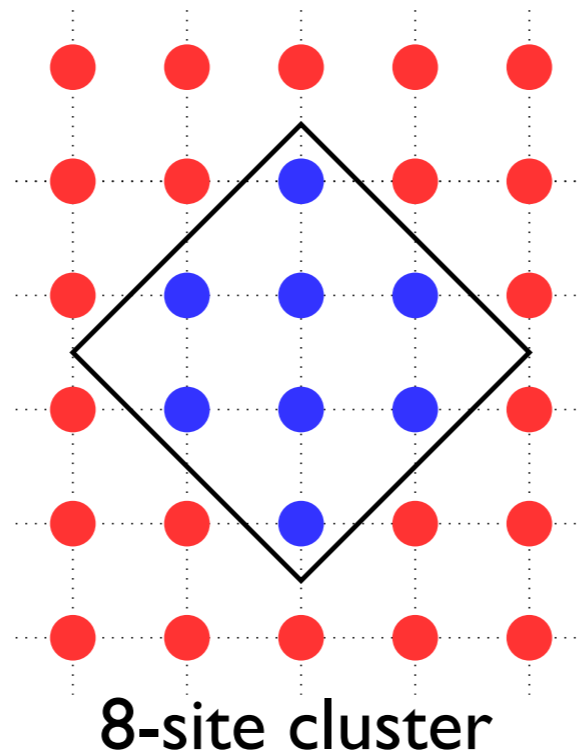
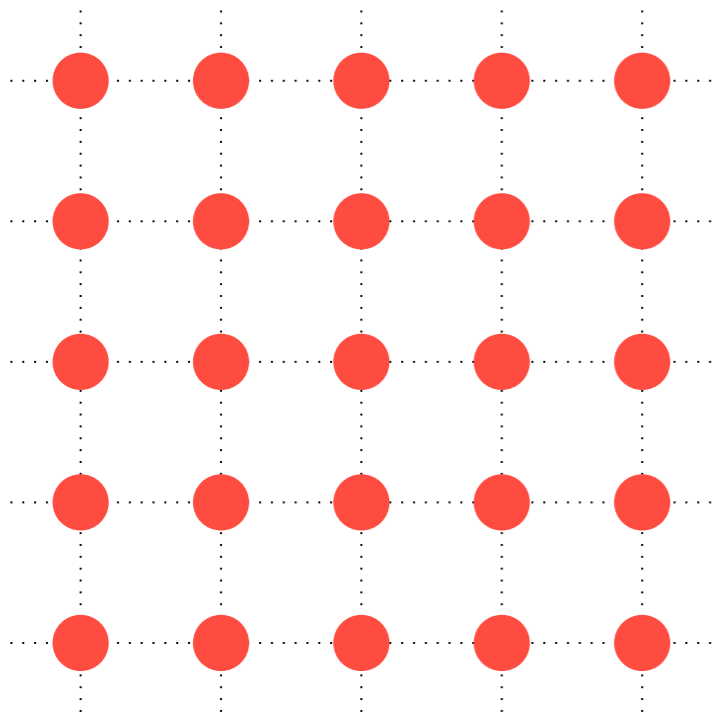
8-site (cluster): clear **node** / **antinode** distinction. Regions away from the Fermi surface (at zero and (π, π)) are not mixed in with regions around the FS.

Cluster Dynamical Mean Field Theory

Maier et al., Rev. Mod. Phys. 77, 1027 (2005)

Hubbard model on
2d square lattice:

$$H = - \sum_{\langle ij \rangle, \sigma} t_{ij} (c_{i\sigma}^\dagger c_{j\sigma} + c_{j\sigma}^\dagger c_{i\sigma}) + U \sum_i n_{i\uparrow} n_{i\downarrow}.$$



Tiling of the BZ

DCA: Hettler et al.,
Phys. Rev. B 58, R 7475 (1998)

Restriction to paramagnetic bath

$$\epsilon_p = -2t(\cos(p_x) + \cos(p_y)) - 4t' \cos(p_x) \cos(p_y)$$

DCA self energy is chosen to be constant within patches of the Brillouin zone.

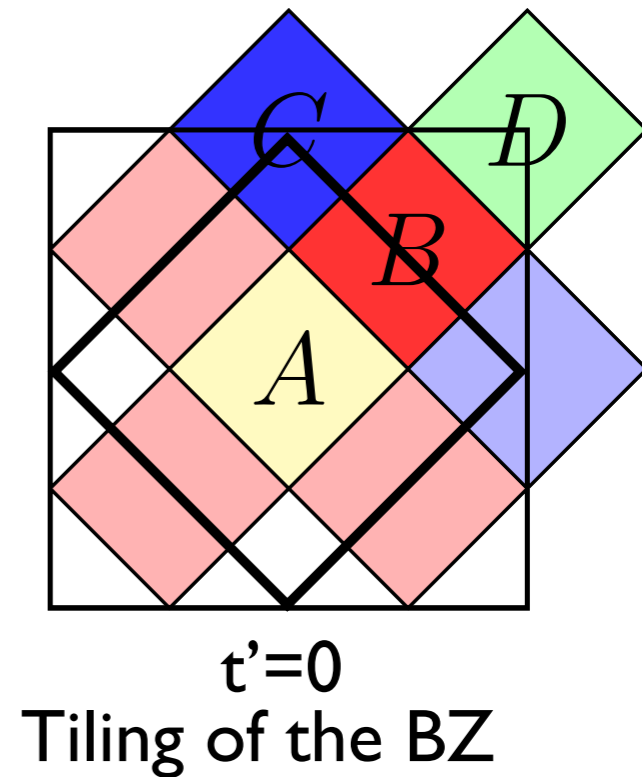
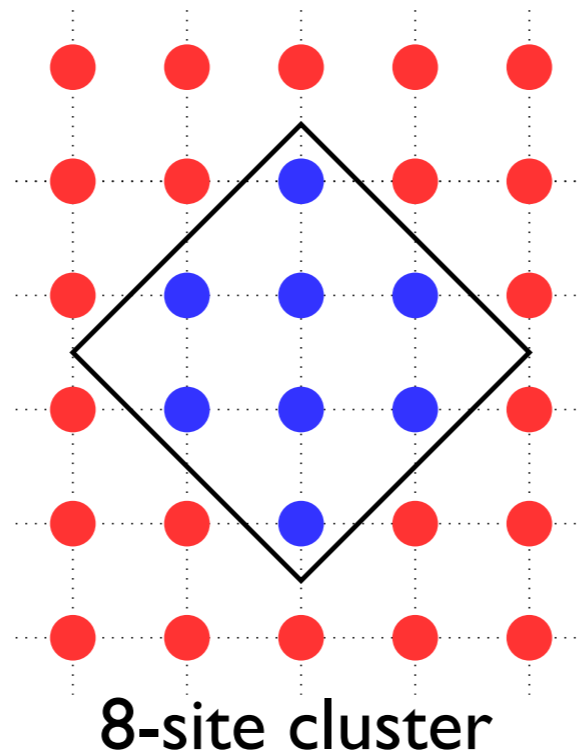
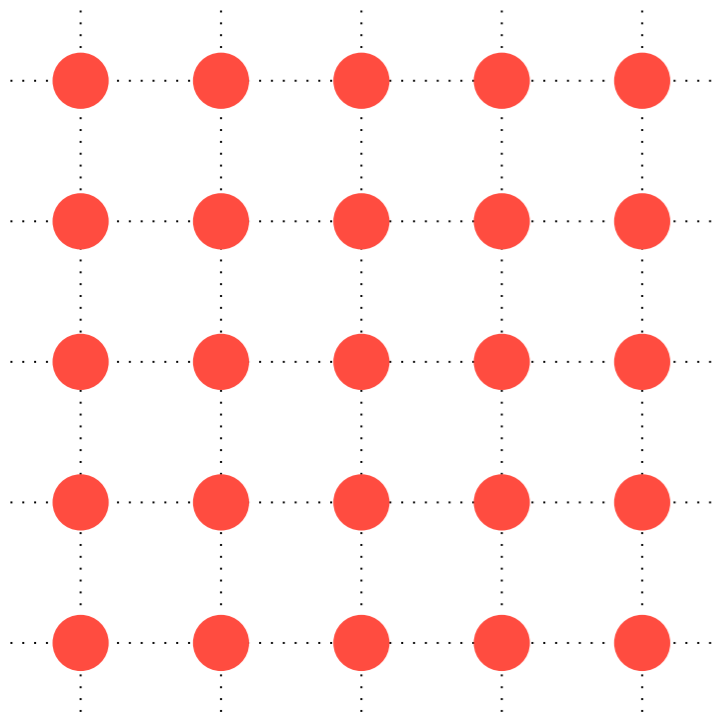
8-site (cluster): clear **node** / **antinode** distinction. Regions away from the Fermi surface (at zero and (π, π)) are not mixed in with regions around the FS.

Cluster Dynamical Mean Field Theory

Maier et al., Rev. Mod. Phys. 77, 1027 (2005)

Hubbard model on
2d square lattice:

$$H = - \sum_{\langle ij \rangle, \sigma} t_{ij} (c_{i\sigma}^\dagger c_{j\sigma} + c_{j\sigma}^\dagger c_{i\sigma}) + U \sum_i n_{i\uparrow} n_{i\downarrow}.$$



DCA: Hettler et al.,
Phys. Rev. B 58, R 7475 (1998)

Restriction to paramagnetic bath

$$\epsilon_p = -2t(\cos(p_x) + \cos(p_y)) - 4t' \cos(p_x) \cos(p_y)$$

DCA self energy is chosen to be constant within patches of the Brillouin zone.

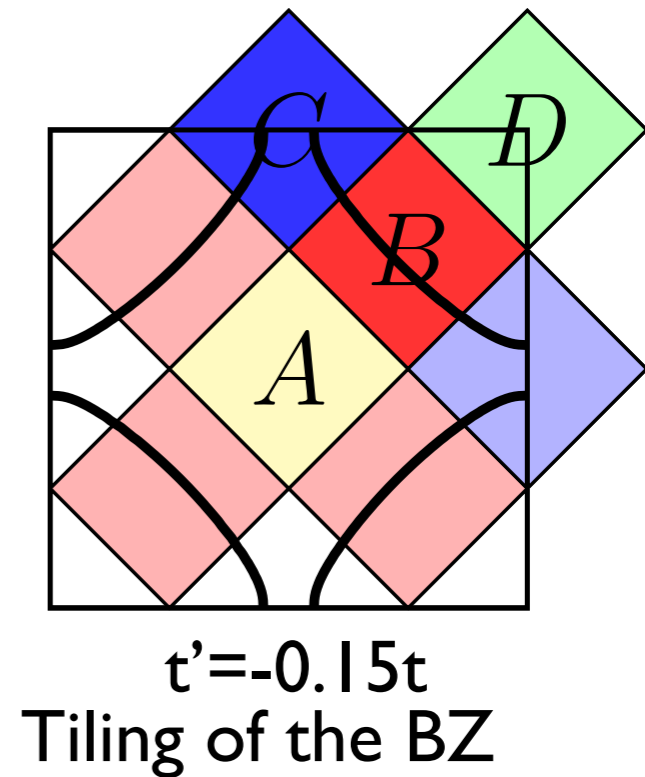
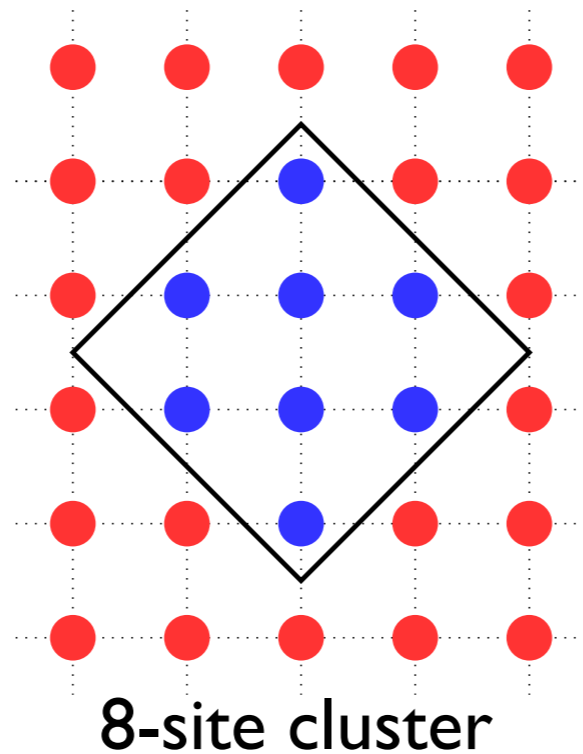
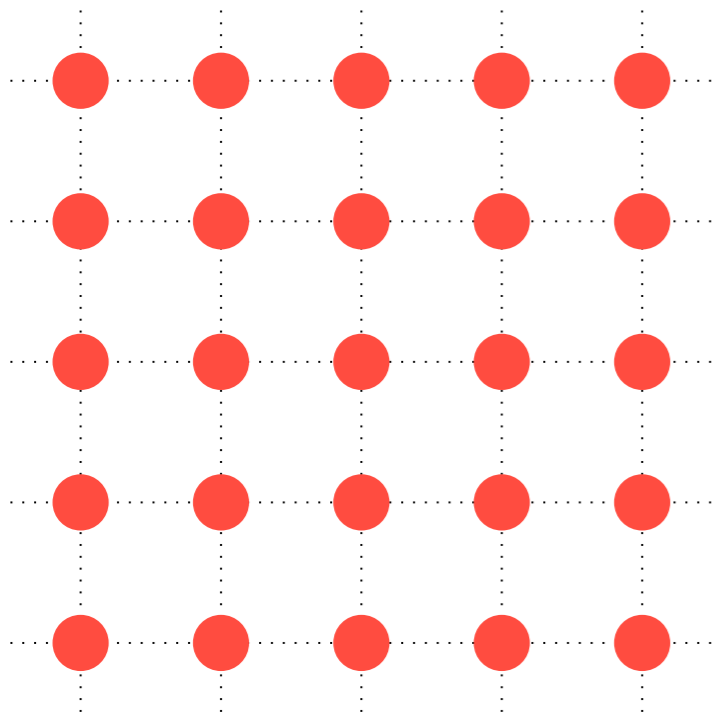
8-site (cluster): clear **node** / **antinode** distinction. Regions away from the Fermi surface (at zero and (π, π)) are not mixed in with regions around the FS.

Cluster Dynamical Mean Field Theory

Maier et al., Rev. Mod. Phys. 77, 1027 (2005)

Hubbard model on
2d square lattice:

$$H = - \sum_{\langle ij \rangle, \sigma} t_{ij} (c_{i\sigma}^\dagger c_{j\sigma} + c_{j\sigma}^\dagger c_{i\sigma}) + U \sum_i n_{i\uparrow} n_{i\downarrow}.$$



DCA: Hettler et al.,
Phys. Rev. B 58, R 7475 (1998)

Restriction to paramagnetic bath

$$\epsilon_p = -2t(\cos(p_x) + \cos(p_y)) - 4t' \cos(p_x) \cos(p_y)$$

DCA self energy is chosen to be constant within patches of the Brillouin zone.

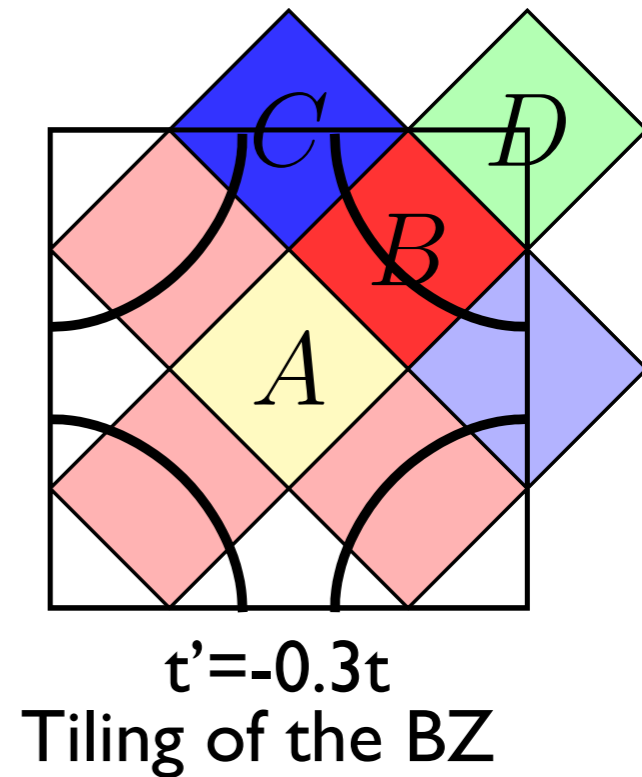
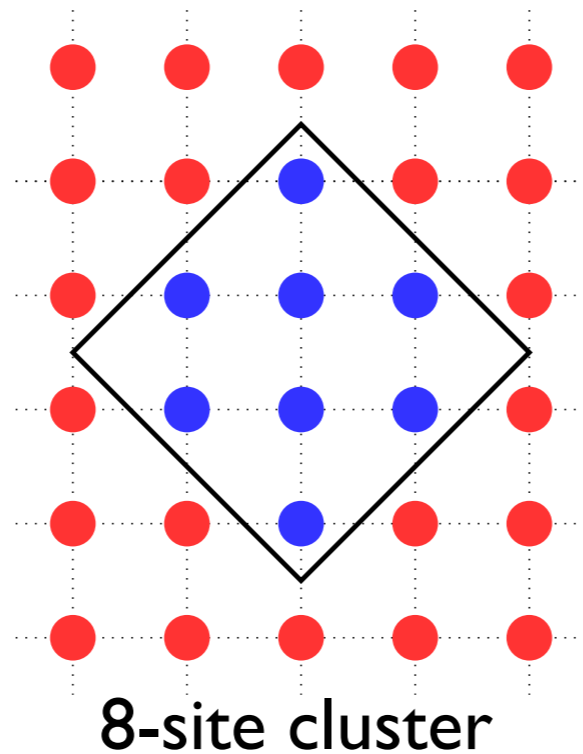
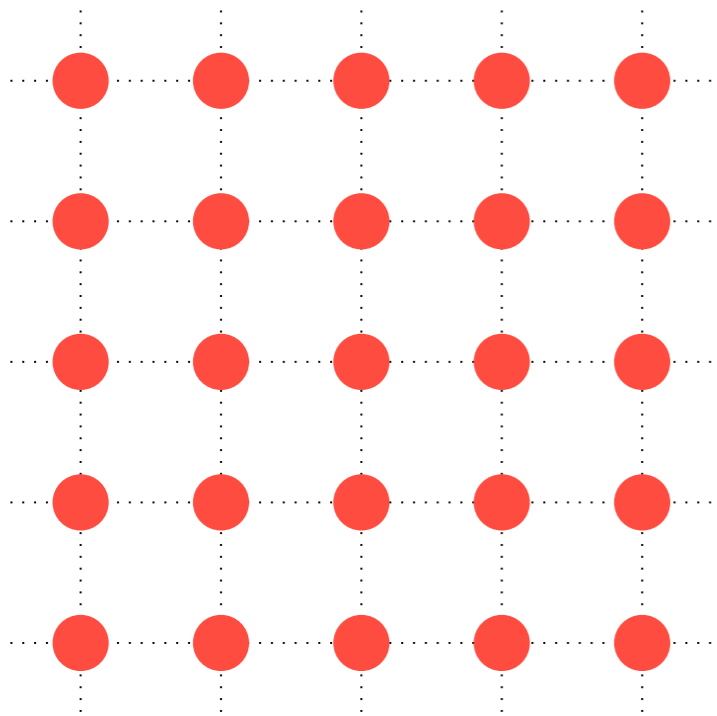
8-site (cluster): clear **node** / **antinode** distinction. Regions away from the Fermi surface (at zero and (π, π)) are not mixed in with regions around the FS.

Cluster Dynamical Mean Field Theory

Maier et al., Rev. Mod. Phys. 77, 1027 (2005)

Hubbard model on
2d square lattice:

$$H = - \sum_{\langle ij \rangle, \sigma} t_{ij} (c_{i\sigma}^\dagger c_{j\sigma} + c_{j\sigma}^\dagger c_{i\sigma}) + U \sum_i n_{i\uparrow} n_{i\downarrow}.$$



DCA: Hettler et al.,
Phys. Rev. B 58, R 7475 (1998)

Restriction to paramagnetic bath

$$\epsilon_p = -2t(\cos(p_x) + \cos(p_y)) - 4t' \cos(p_x) \cos(p_y)$$

DCA self energy is chosen to be constant within patches of the Brillouin zone.

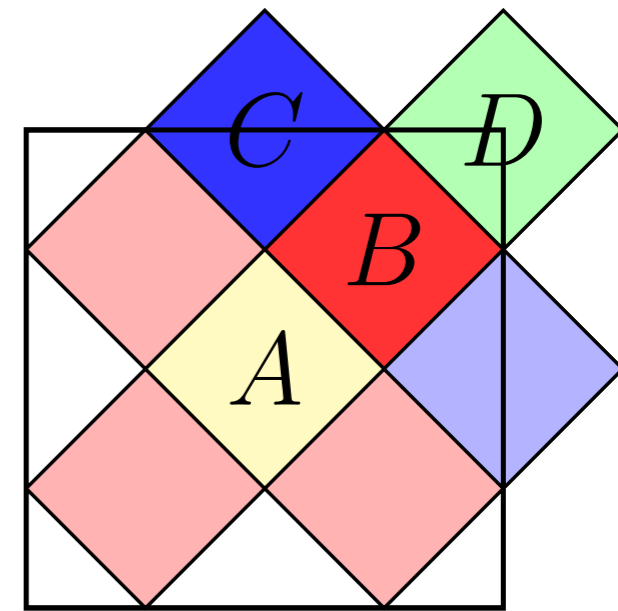
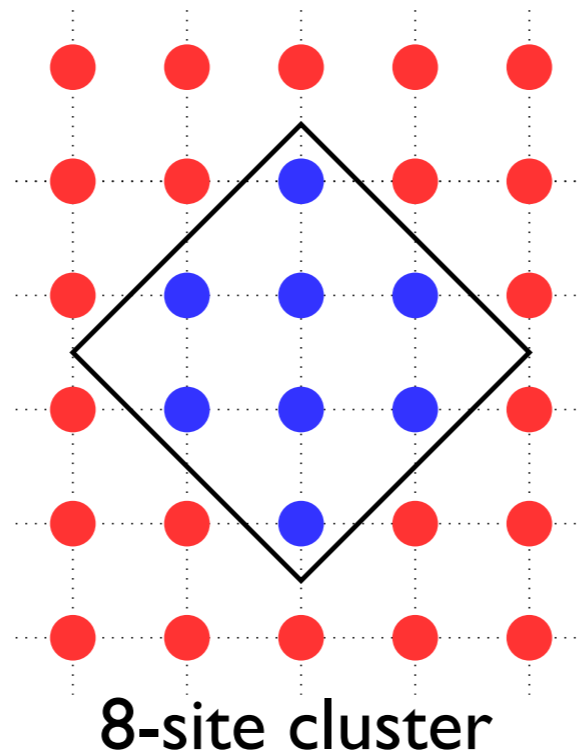
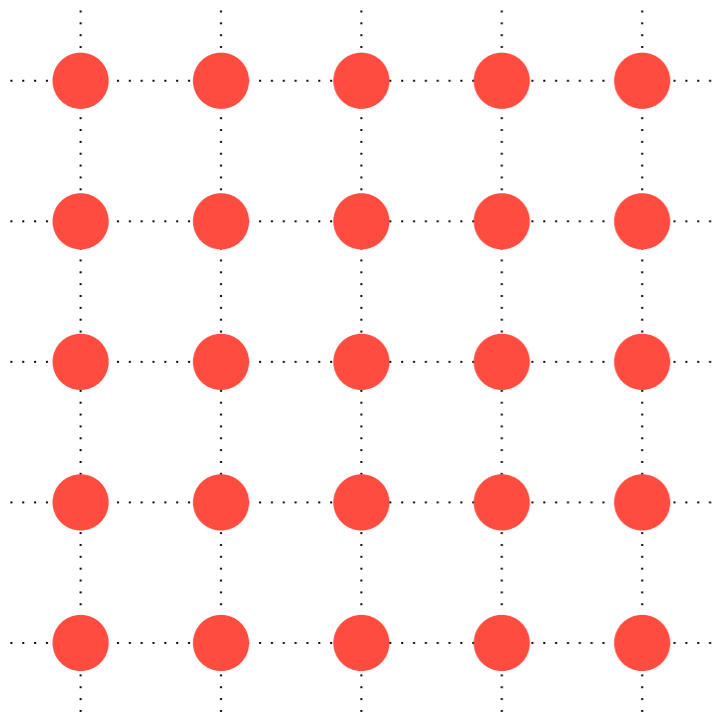
8-site (cluster): clear **node** / **antinode** distinction. Regions away from the Fermi surface (at zero and (π, π)) are not mixed in with regions around the FS.

Cluster Dynamical Mean Field Theory

Maier et al., Rev. Mod. Phys. 77, 1027 (2005)

Hubbard model on
2d square lattice:

$$H = - \sum_{\langle ij \rangle, \sigma} t_{ij} (c_{i\sigma}^\dagger c_{j\sigma} + c_{j\sigma}^\dagger c_{i\sigma}) + U \sum_i n_{i\uparrow} n_{i\downarrow}.$$



Tiling of the BZ

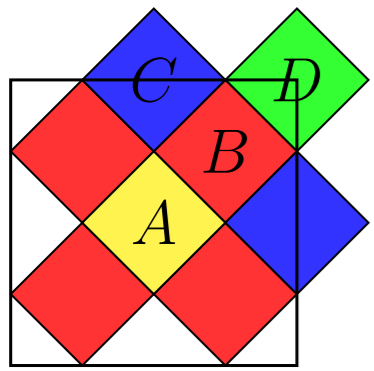
DCA: Hettler et al.,
Phys. Rev. B 58, R 7475 (1998)

Restriction to paramagnetic bath

$$\epsilon_p = -2t(\cos(p_x) + \cos(p_y)) - 4t' \cos(p_x) \cos(p_y)$$

DCA self energy is chosen to be constant within patches of the Brillouin zone.

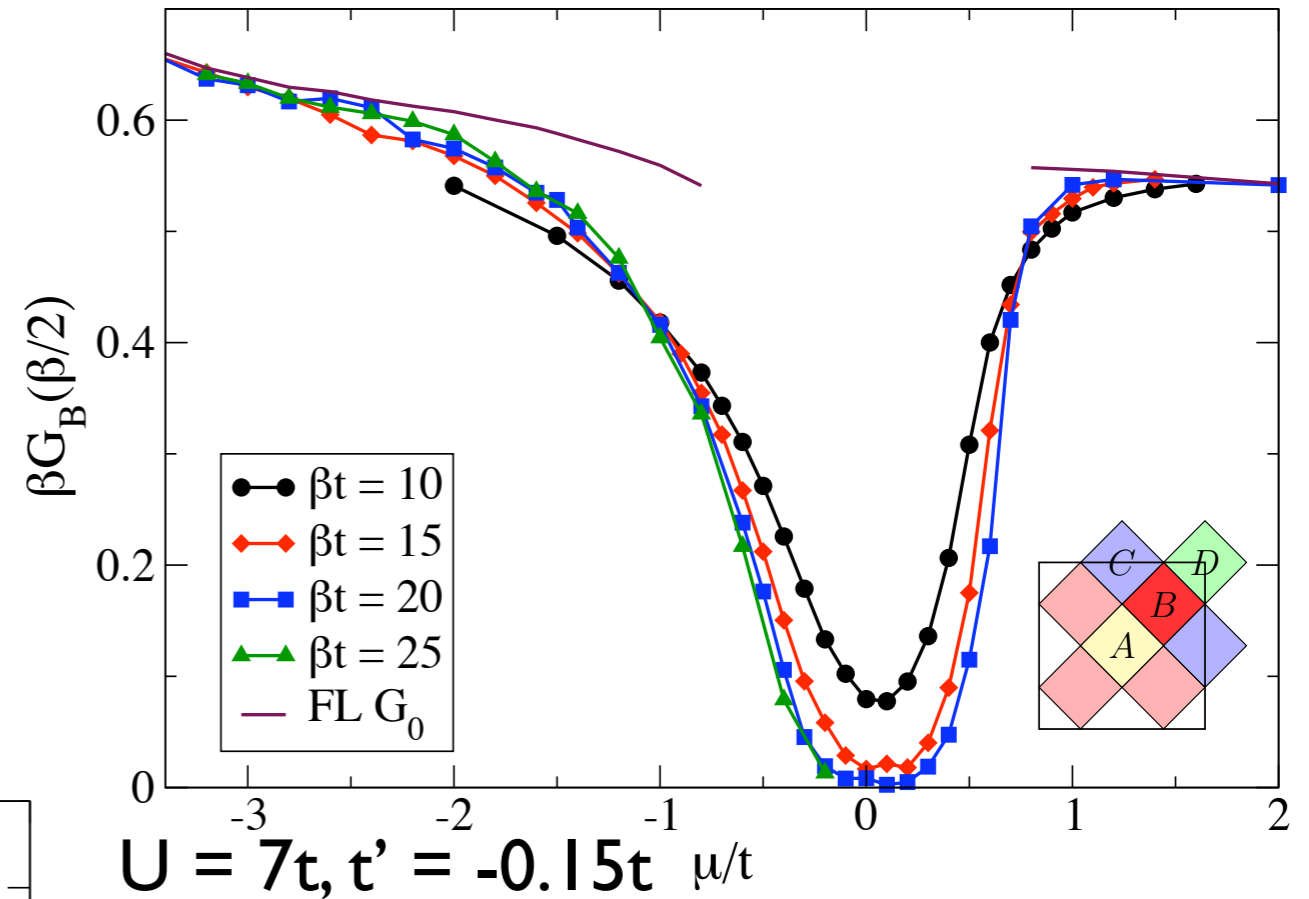
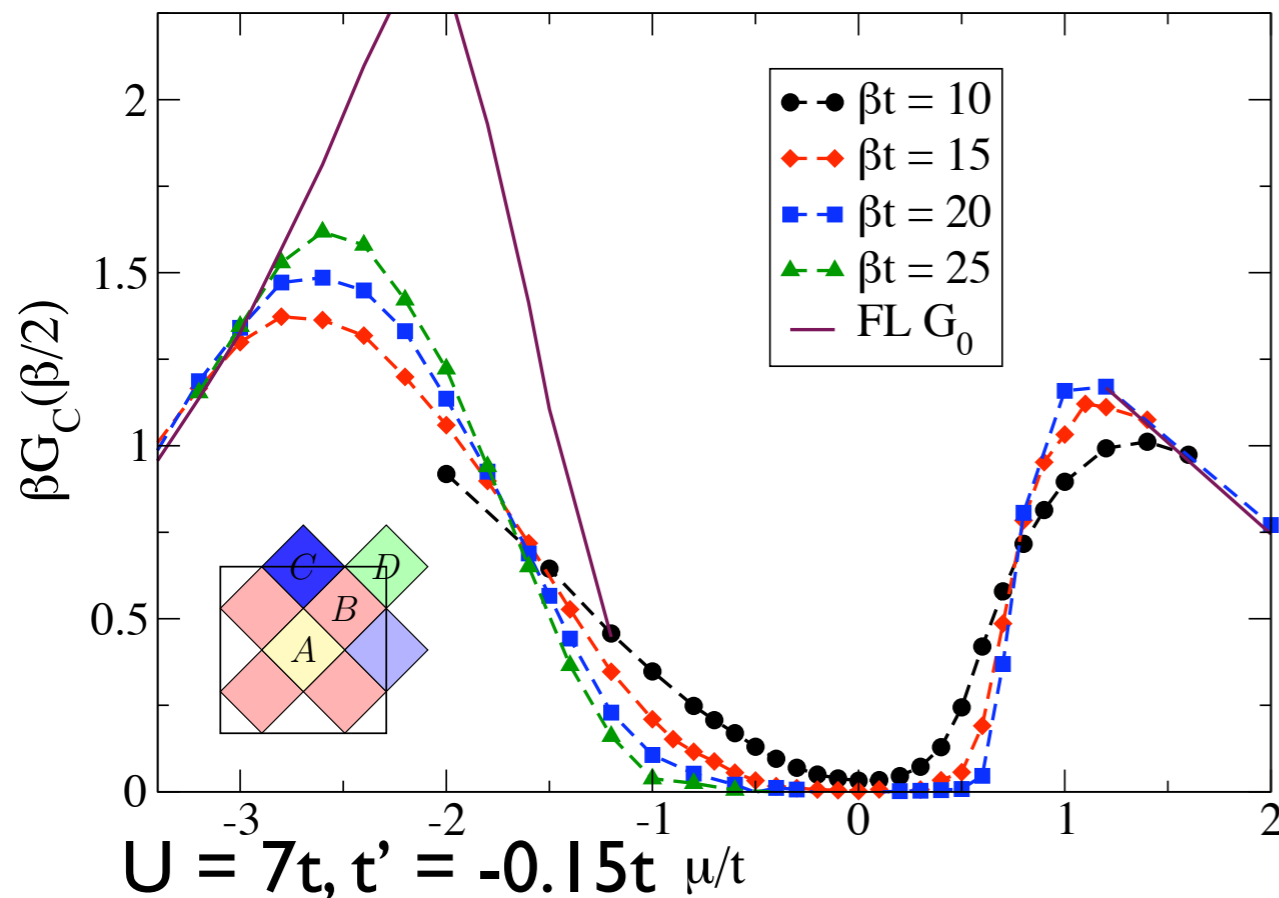
8-site (cluster): clear **node** / **antinode** distinction. Regions away from the Fermi surface (at zero and (π, π)) are not mixed in with regions around the FS.



Results: Doping Driven Transition

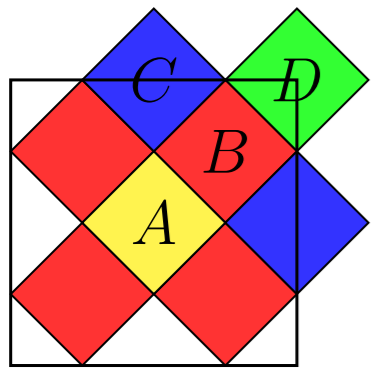
Spectral function $A(0)$ at the Fermi energy as a function of chemical potential exhibits clear crossing points.

Sector **C** transition occurs before sector **B** transition. Transitions coalesce on the electron doped side for larger t' , but not on the hole doped side.



For large electron and hole doping:
 behavior consistent with Fermi liquid theory.

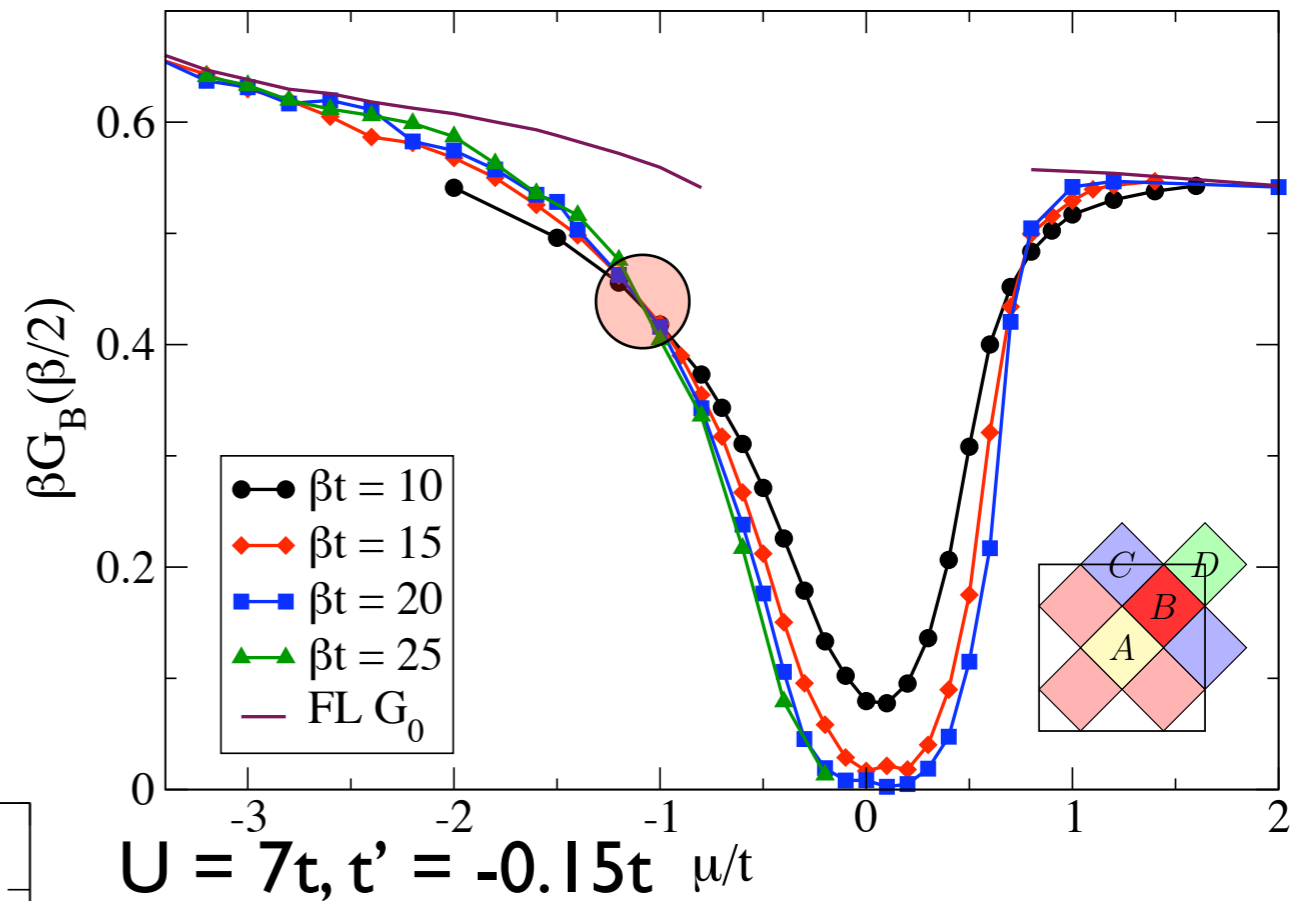
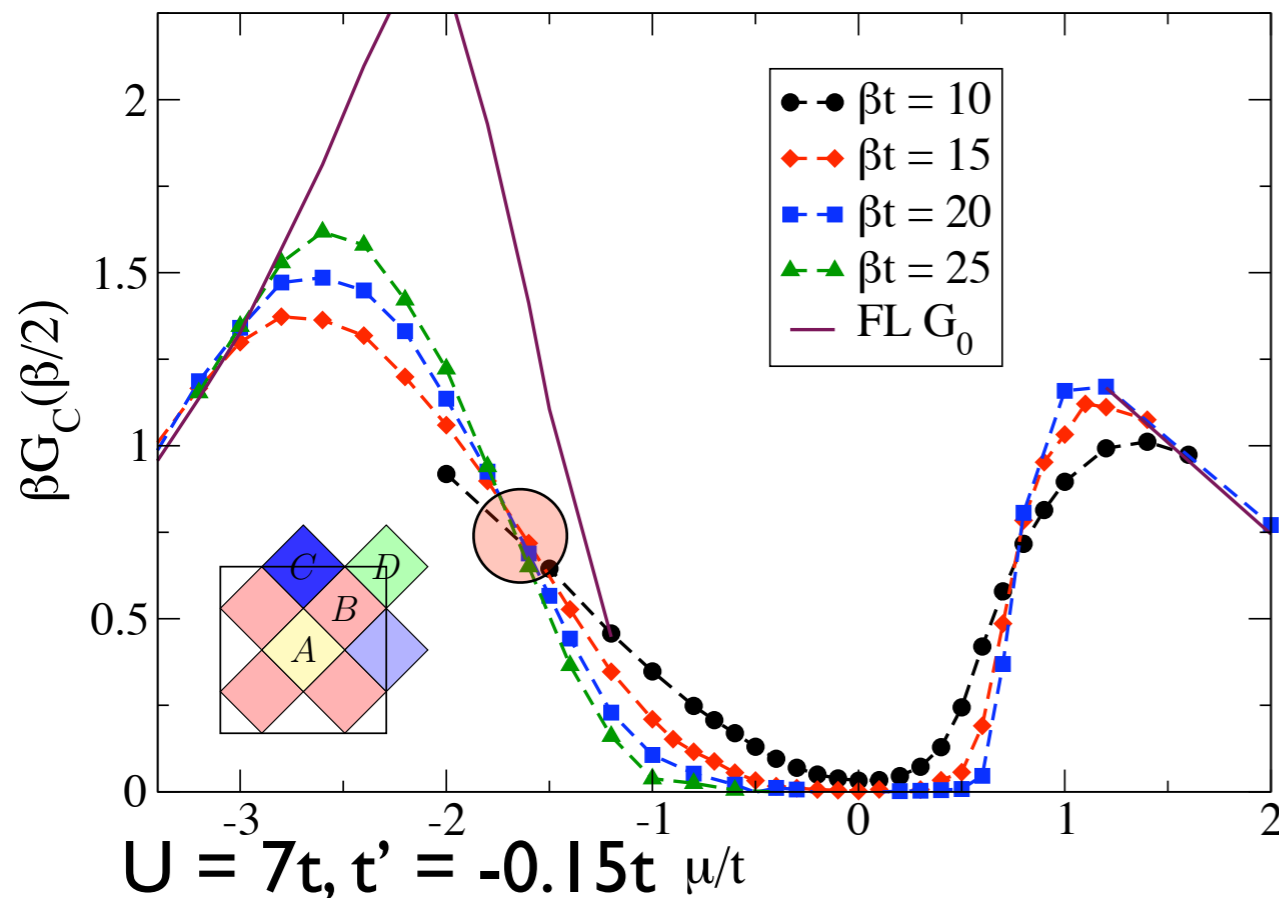
For intermediate doping: $A(0)$ is suppressed in comparison with FL, possible Non-FL phase in sector B.



Results: Doping Driven Transition

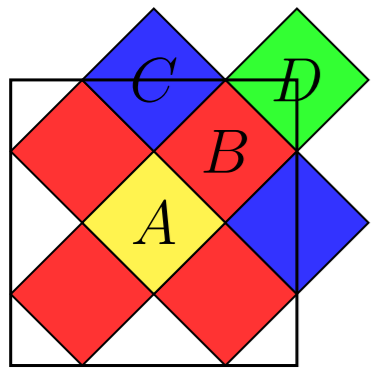
Spectral function $A(0)$ at the Fermi energy as a function of chemical potential exhibits clear crossing points.

Sector **C** transition occurs before sector **B** transition. Transitions coalesce on the electron doped side for larger t' , but not on the hole doped side.



For large electron and hole doping: behavior consistent with Fermi liquid theory.

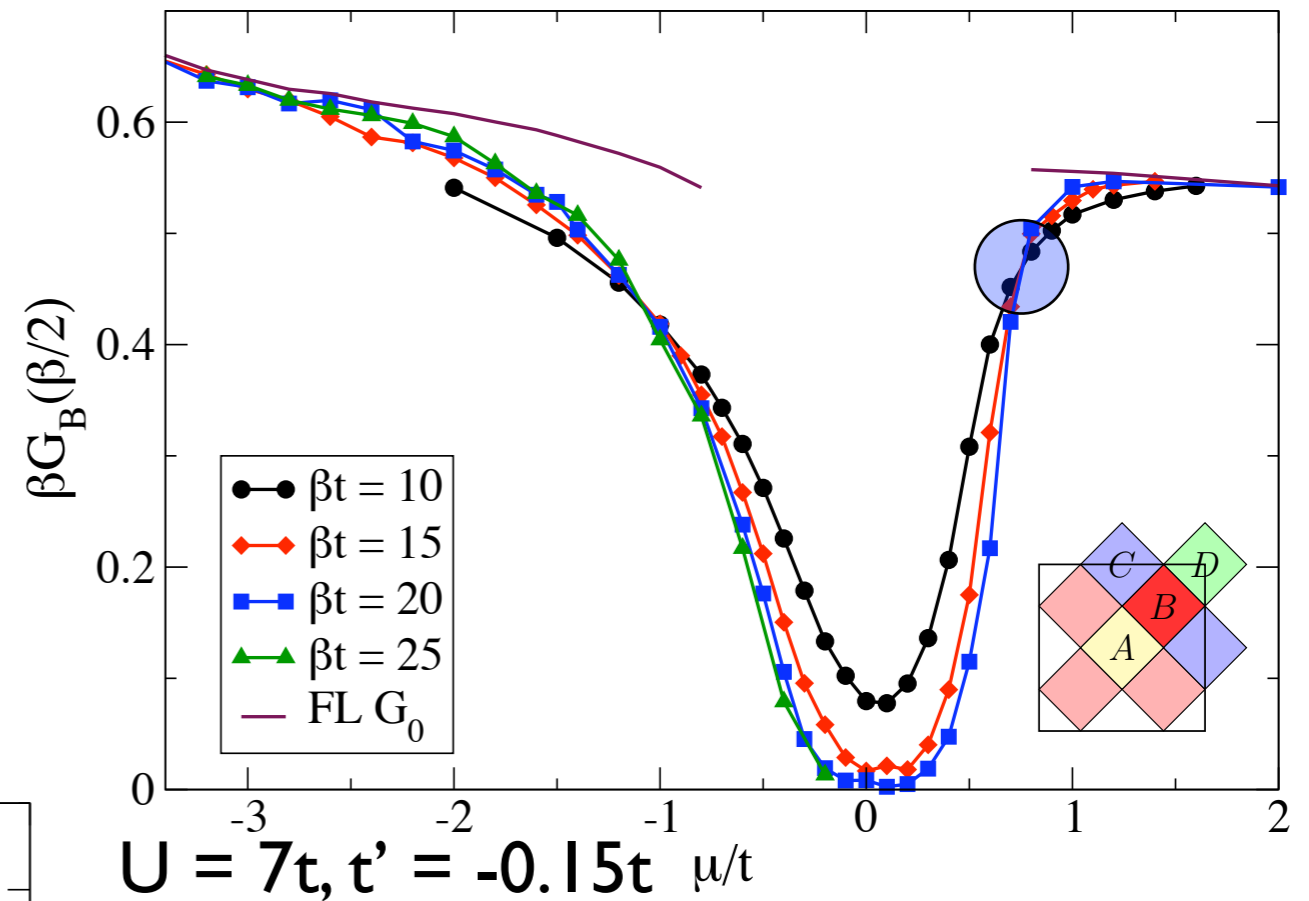
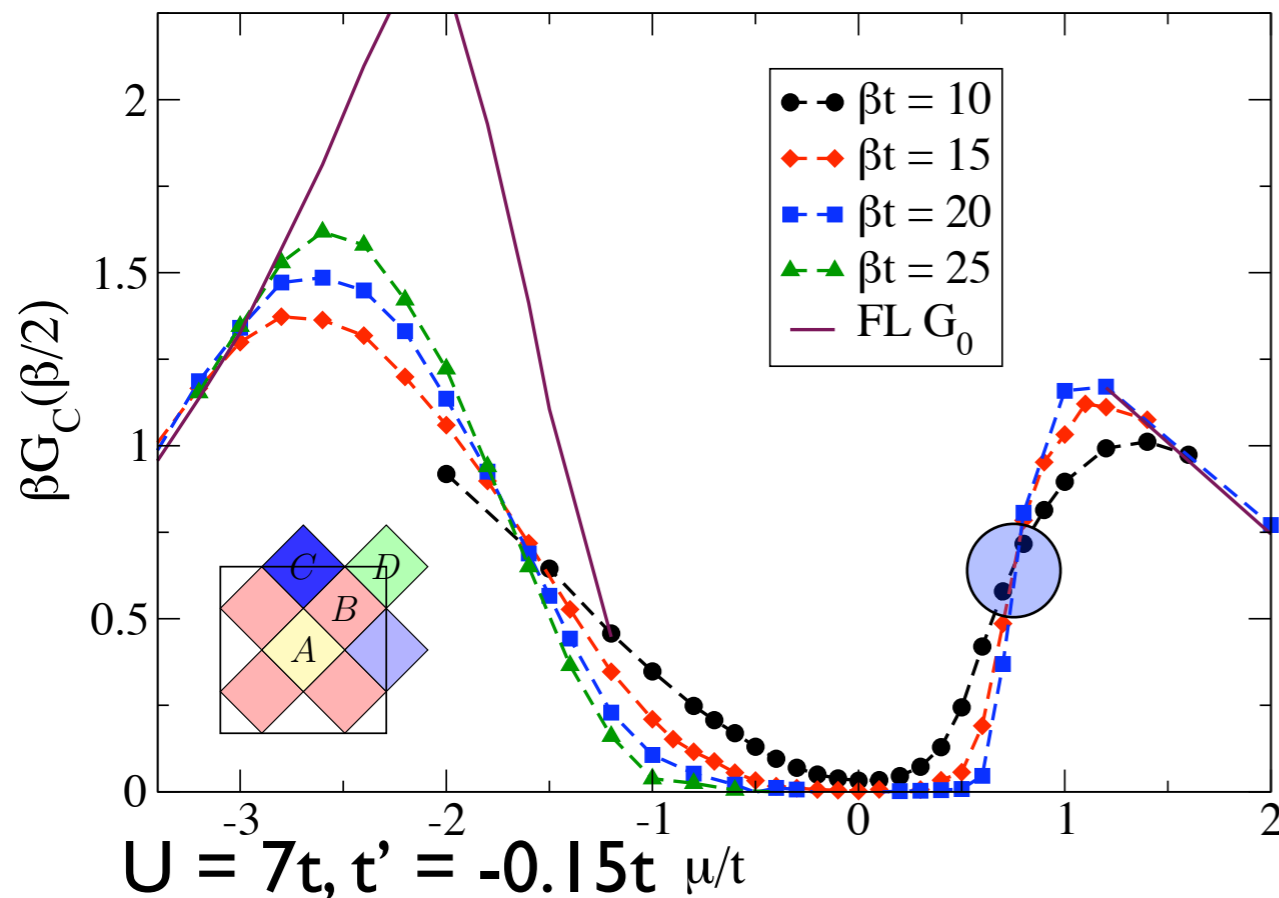
For intermediate doping: $A(0)$ is suppressed in comparison with FL, possible Non-FL phase in sector B.



Results: Doping Driven Transition

Spectral function $A(0)$ at the Fermi energy as a function of chemical potential exhibits clear crossing points.

Sector **C** transition occurs before sector **B** transition. Transitions coalesce on the electron doped side for larger t' , but not on the hole doped side.



For large electron and hole doping: behavior consistent with Fermi liquid theory.

For intermediate doping: $A(0)$ is suppressed in comparison with FL, possible Non-FL phase in sector B.

Conclusions

For a review on continuous-time algorithms see my PhD thesis
<http://e-collection.ethbib.ethz.ch/view/eth:31103>

Open source codes: In preparation, will be published this summer as part of the ALPS (alps.comp-phys.org) libraries.

New algorithms allow access to **new physics**: **Larger systems**, extrapolation to the **infinite system**, **general interactions**, and **more orbitals**.

